Transportation Research Part C 71 (2016) 464–488

Contents lists available at ScienceDirect

Transportation Research Part C

journal homepage: www.elsevier.com/locate/trc

Optimal vehicle trajectory planning in the context of cooperative merging on highways

Ioannis A. Ntousakis, Ioannis K. Nikolos *, Markos Papageorgiou

School of Production Engineering and Management, Technical University of Crete, University Campus, GR-73100 Chania, Greece

ARTICLE INFO

Article history:
Received 11 January 2016
Received in revised form 18 April 2016
Accepted 11 August 2016
Available online 1 September 2016

Keywords:
Optimal vehicle trajectory planning
Cooperative merging
Automated vehicles
Connected vehicles
Model Predictive Control

ABSTRACT

One of the main triggers of traffic congestion on highways is vehicle merging at on-ramps. The development of automated procedures for cooperative vehicle merging is aimed to ensure safety and alleviate congestion problems. In this work, a longitudinal trajectory planning methodology is presented, developed to assist the merging of vehicles on highways; it achieves safe and traffic-efficient merging, while minimizing the engine effort and passenger discomfort through the minimization of acceleration and its first and second derivatives during the merging maneuver. The problem is formulated as a finite-horizon optimal control problem and is solved analytically. This enables the solution to be stored on-board, saving computational time and rendering the methodology suitable for practical applications. The tunable weights, used for taking into account the different optimization criteria, may serve as parameters to match the individual driver's preferences. The proposed methodology is first developed for a pair of cooperating vehicles, a merging one and its putative leader. Moreover, an alternative solution procedure via a time-variant Linear-Quadratic Regulator approach is also presented. A Model Predictive Control (MPC) scheme is utilized to compensate possible disturbances in the trajectories of the cooperating vehicles, whereby the analytical optimal solution is applied repeatedly in real time, using updated measurements, until the merging procedure is actually finalized. Subsequently, the methodology is generalized for a set of vehicles inside the merging area. Various numerical simulations illustrate the validity and applicability of the method.

1. Introduction

The merging of mainstream traffic flow with the incoming flow at on-ramps is a major trigger of traffic flow problems on highways, such as speed breakdown, traffic flow oscillations and congestion (Davis, 2006; Pueboobpaphan et al., 2010; Milanés et al., 2011; Marczak et al., 2013; Sun et al., 2014). Moreover, in manual driving, the merging maneuvers may be stressful due to the involved risk, the close interaction with other drivers, and the requirement for a good synchronization of observations, calculations and actions in a very short time window. As the interacting cars and drivers in the merging procedure have, in general, different abilities, characteristics, and driving styles, the merging process is often performed inefficiently with respect to the traffic flow and throughput, but also with respect to passengers' safety and comfort (Tideman et al., 2007). To this end, a continuously increasing effort is spent for the development of merging assistance systems, as part

* Corresponding author.
E-mail address: jnikolo@dpem.tuc.gr (I.K. Nikolos).

http://dx.doi.org/10.1016/j.trc.2016.08.007
0968-090X/

of the development of a class of Vehicle Automation and Communication Systems (VACS), to enable cooperative merging of equipped vehicles (Tideman et al., 2007; Pueboobpaphan et al., 2010; Scarinci and Heydecker, 2014).

The proposed algorithms for cooperative merging share common characteristics, but also have major differences, for example in the adopted assumptions, the network layout, the type of vehicles and their level of "intelligence", the type and location of the control, the type of communications, etc. The layout of the networks may include single or multiple lanes in each stream. Although the most efficient merging requires the coordination of both mainstream and on-ramp vehicles, control algorithms exist, which control only the one stream of vehicles. Centralized or decentralized control can be used; in the first case, the decisions are taken in a traffic management center, while in the second case the decisions are made on each individual vehicle, and may transmitted to the affected vehicles (Scarinci and Heydecker, 2014).

Before proceeding to the application of the automated merging maneuvers, a merging sequence must be established first, which refers to the specific sequence of vehicles from the two streams when passing through the merging area. Several criteria can be used to define the merging sequence, such as safety, passenger comfort, flow efficiency, fuel consumption and emissions, time delay, etc. The creation of the merging sequence should be the result of an upper-level controller, while the lower-level merging controller is dedicated to the merging maneuvers for each involved vehicle. In his work back in 1969, Athans (Athans, 1969) formulated the merging problem as an optimal control problem for a given merging sequence; all possible sequences are evaluated and the optimal one is selected. Thereafter, several works have been published for the creation of the merging sequence (see for example Posch and Schmidt, 1983; Li et al., 2007; Cao et al., 2014; Ntousakis et al., 2014a).

In general, the lower-level merging controller has two distinct tasks: firstly the creation of the proper gap; and secondly the control of the speeds of the cooperating vehicles to produce an efficient and safe merging (Pueboobpaphan et al., 2010). The control of the affected vehicles and the computation of the merging trajectories has been the subject of several papers. In Posch and Schmidt (1983) two different algorithms are proposed: a conflict and a non-conflict one. In the second one, vehicles are not predicted to violate safety constraints, and a heuristic strategy is applied for the computation of a constant acceleration. In the first algorithm, the putative follower assumes that the leader follows the non-conflict mode, while its own speed is controlled using a modified reference trajectory. Three control guidance laws have been proposed in Kachroo and Li (1997), with linear, "optimal", and parabolic velocity profiles, respectively, for the merging vehicle, using sliding mode control theory. The "optimal" velocity profile is defined in the sense of minimizing acceleration deviations. In Ran et al. (1999), the proposed control strategy aims to match on-ramp merging vehicles to specifically created (or adjusted) gaps in the mainstream; an upper level controller is used for assigning the gaps to the merging vehicles, so that vehicles can merge at the mainline speed. Several sub-models are used to provide the speed profile of the merging and mainstream vehicles, namely "platoon forming", "platoon following", "check for gap", "gap adjustment", "gap assignment", and "deceleration for metering".

In the merging algorithm presented in Lu et al. (2004), a virtual platoon is formed before the on-ramp merging vehicle arrives at the merging point; speed and acceleration of the merging vehicle are the same as those of the platoon vehicles in the mainstream; the distance of the merging vehicle to the merging point equals the distance of the corresponding merging slot to the same point. In Davis (2006), an algorithm was proposed, which utilizes a virtual vehicle, imitating the movement of the preceding vehicle in the adjacent lane; the purpose of the additional introduced interactions, which are of a car-following nature, is to adjust headways so that safe distances in front of and behind the merging vehicle are obtained before reaching the merging point. The algorithm was later adapted and evaluated for a mixed traffic environment with different penetration rates of ACC (Adaptive Cruise Control)-equipped vehicles (Davis, 2007), demonstrating a considerable improvement in throughput due to the cooperative merging. In Li et al. (2007) a trajectory planning algorithm was developed for lane closures, controlling both longitudinal and lateral movements, using fifth order polynomials.

In Raravi et al. (2007) an optimization problem was formulated with the objective to minimize the time taken by vehicles to reach the intersection region, subject to safety-related constraints; additionally a head-of-lane algorithm was proposed for achieving the same goal with less computational overhead. In Pueboobpaphan et al. (2010) a decentralized merging assistant was proposed, applicable in mixed traffic situations, designed to increase flow stability by minimizing conflicts in the merging region and limiting the speed changes. CACC-equipped vehicles are assumed in the mainstream, while a roadside unit (RSU) predicts the time the ramp vehicle needs to arrive at the acceleration lane. The mainstream CACC (Cooperative Adaptive Cruise Control) vehicles decelerate well in advance to avoid being within a safety zone of the on-ramp merging vehicles. A driver-assistance system for controlling the longitudinal motion of both on-ramp and mainstream vehicles was proposed in Milanés et al. (2011) for congested traffic, having as objectives to avoid congestion on the on-ramp and to minimize the effect of the on-ramp merging vehicles on the congested mainstream. The virtual vehicle concept is used to map the merging vehicle on the mainstream, while the control is based on fuzzy logic, applied and tested to actual vehicles in low speeds. In Park et al. (2011) an algorithm was developed for providing lane-changing advisories to mainstream vehicles to create space for the on-ramp merging ones, using variable gap sizes, according to the speeds and characteristics of vehicles.

In Rios-Torres et al. (2015) an analytic solution is developed for the problem of coordinating connected vehicles traveling over two merging roads. The problem is formulated as an optimal control problem aiming to find a safe and fuel-efficient crossing schedule for all the vehicles in the control zone; acceleration is used in the objective function of the related optimal control problem.

A trajectory planning methodology is developed in this work, to enable automated merging of mainstream and single-lane on-ramp vehicles onto a single-lane mainstream. The designed trajectories minimize the engine effort and passenger discomfort by minimizing vehicle acceleration, jerk and its first derivative. The minimization of acceleration is directly

connected to the minimization of fuel consumption (Rios-Torres et al., 2015). On the other hand, as stated in Elbanhawi et al. (2015), optimizing the movement of the vehicle to minimize resulting forces and jerk acting on the passengers, is the most common approach towards passenger comfort. Thus, in a different (non-merging) context, (Rathgerber et al., 2015) use the longitudinal and lateral jerk for calculating optimal vehicle trajectories to maximize passengers' comfort; while, in an alternative simplified approach, the derivative of the jerk is also used to produce optimal trajectories described with polynomials of 7th order.

Another purpose for the proposed methodology is to enable efficient merging with respect to the resulting total outflow, by ensuring pre-specified time-headways and vehicle speeds at the end of the maneuver, which correspond to maximum throughput. A finite-horizon optimal control problem with fixed final states is formulated to this end, and solved analytically. Tunable weights are used for combining the different optimization criteria, which may also serve as parameters to be tuned by the drivers according to their preferences. Initially, a pair of cooperating vehicles is used for the development of the methodology, while a Model Predictive Control scheme is established to compensate possible disturbances in the trajectories of the cooperating vehicles, by using updated real-time measurements in each time step for the formation of the remaining part of the optimal trajectory. Then, the methodology is further developed and tested for a set of vehicles inside the merging area.

The paper is structured as follows: in Section 2, the merging control framework is presented. In Section 3, the optimal control problem is defined for a pair of vehicles (a merging one and its putative leader), while analytic solutions are derived for: (a) the minimization of acceleration alone, (b) the minimization of the jerk alone, and (c) the minimization of the first time-derivative of jerk of the merging vehicle. In Section 4, an analytic solution for a combined cost function is derived, which includes the minimization of acceleration, jerk and the first derivative of jerk. Additionally, a discrete-time Quadratic Programming formulation, which allows for explicit consideration of inequality constraints, is presented. The effect of the relative weight values on the shape of the produced trajectory are illustrated and discussed. Moreover, an alternative solution procedure via a time-variant LQR (Linear-Quadratic Regulator) approach is also offered. The lateral movement of on-ramp vehicles is finally discussed. In Section 5, the MPC framework is presented and applied to specific examples; furthermore, it is compared to a typical ACC-based system. Subsequently, the MPC framework is further generalized for a set of vehicles. In Section 6, the concluding remarks are presented, while in Appendix A, the linear system of equations which provide the expressions for the constants involved in the various analytic solutions of the optimal control problem, are included.

2. The merging control framework

Typically, the merging process for an on-ramp driver includes a set of coordinated tasks. Firstly, the driver scans the adjacent target lane for possible gaps and evaluates which gap is the best one according to her preferences (e.g. the safest, the most comfortable, the first available, etc.). Once the gap is selected, the driver adjusts accordingly the speed of her vehicle to align with the targeted gap and mainstream vehicle speed; and, finally, performs the required maneuvers to merge. The purpose of the proposed methodology is to produce trajectories for the involved (on-ramp and mainstream) vehicles that will make the speed adjustment and gap alignment process optimal, as far as traffic efficiency, the applied vehicle effort and the passenger comfort are concerned.

In this work, a single mainstream motorway lane is considered, with a single-lane on-ramp leading to an acceleration lane, as illustrated in Fig. 1. We define the merging point close to the end of the acceleration lane, where the merging vehicles coming from the on-ramp will perform the final merging maneuver (incorporating lateral motion also) to enter the mainstream flow. All vehicles coming from the on-ramp are enforced to merge at this point; however, the proposed methodology can be generalized to deal with varying merging points. Further, we define a cooperation area, starting from a pre-specified distance (both on the mainstream and on the on-ramp) upstream of the merging point and ending at the merging point (Fig. 1). Inside this cooperation area, all vehicles (on both the mainstream and the on-ramp) are called merging vehicles and are under merging control. The use of a fixed merging point allows for the longitudinal and lateral movements of vehicles to be treated independently. While the following sections tackle the more crucial longitudinal movement, the lateral movement for on-ramp vehicles is addressed in Section 4.6. For the longitudinal movement, the position of each vehicle inside the cooperation area is defined by its lane (mainstream or on-ramp) and its x-distance from the merging point. In the following, when addressing a specific merging vehicle, we will call it, for brevity and clarity, the ego vehicle.

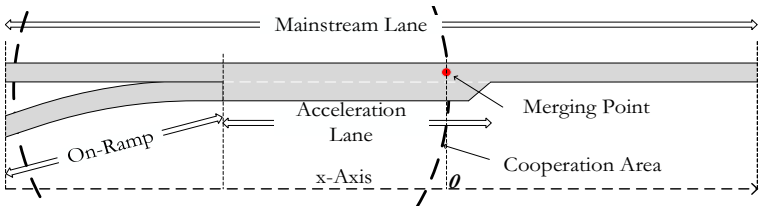

Fig. 1. The topology of the motorway, where the optimal merging trajectory is computed and applied.

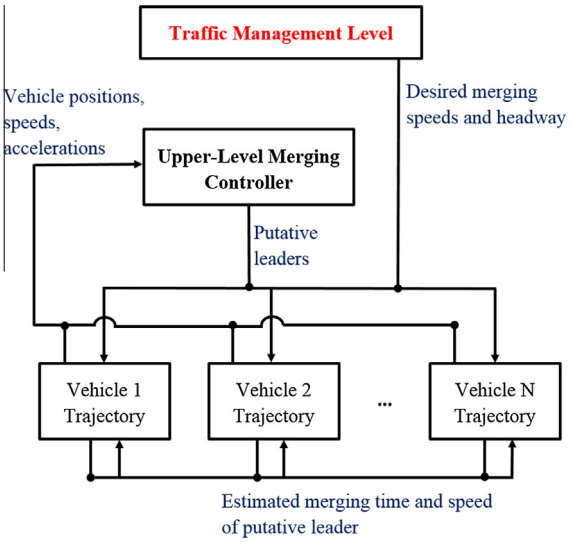

Fig. 2. Schematic representation of all involved control layers.

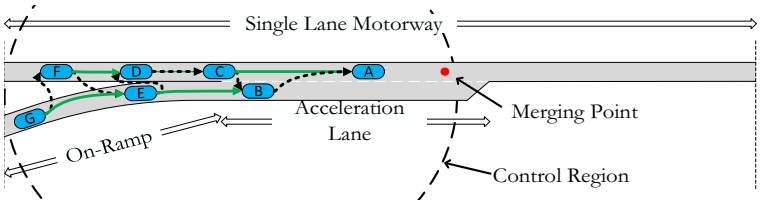

Fig. 3. For each vehicle in the cooperation area, the green solid arrow indicates its physical leader and the dashed black arrow the putative leader; for example, for vehicle C the physical leader is vehicle A, while the putative leader is vehicle B. (For interpretation of the references to colour in this figure legend, the reader is referred to the web version of this article.)

In a typical merging scenario, more than one vehicles will, in general, be present inside the cooperation area at each time instant. Prior to designing the optimal merging trajectories, it is necessary to define the sequence (Merging Sequence - MS) in which the vehicles shall reach the merging point and eventually move downstream of the cooperation area. It is assumed here that an upper control level exists, located either in the traffic control center or in a nearby road side unit (RSU), which performs the determination (and real-time update) of the MS according to appropriate criteria (e.g. current vehicle speeds, possible priority of mainstream versus ramp flow, etc.). This upper-level controller (Fig. 2) updates the MS every time a new vehicle enters or exits the cooperation area, or when the current speeds and positions of the vehicles inside the cooperation area have changed beyond prescribed levels. The MS algorithm and the criteria employed to produce or modify the MS are outside the scope of this work. However, it was demonstrated, e.g. in Ntousakis et al. (2014a), that even relatively simple MS schemes may produce a smooth and efficient total traffic flow at the macroscopic level.

A given MS implies that, for each vehicle inside the cooperation area, a "putative leader" (i.e. the preceding vehicle in the MS) has been assigned (Fig. 3), and this is actually the output of the upper control level; except if no merging conflict is predicted for a vehicle (e.g. because it is the only one or the first to enter in the cooperation area), in which case no putative leader needs to be assigned; such vehicles can continue their movement without any influence from the cooperative merging system. Clearly, with increasing upstream and on-ramp demand, the number of vehicles without a putative leader will be accordingly decreasing or even nullified. The putative leader of a vehicle may or may not be its physical leader (the preceding vehicle in the same lane), as it can be a vehicle of a different lane, as illustrated in Fig. 3.

The physical and the putative leaders of a vehicle influence its movement in a different manner (Fig. 3). Specifically, the putative leader delivers to the ego vehicle appropriate information (merging time and speed estimates) that is used by the ego vehicle in order to design its merging trajectory according to Section 3. On the other hand, the physical leader is taken into account by the vehicle's car-following (ACC) control. The most restrictive of both resulting accelerations is actually applied to the vehicle to guarantee safety under any circumstances. Thus, from the point of view of merging trajectory control, the car-following law may be viewed as a possible disturbance. This treatment of the problem can be applied to each vehicle that arrives in the cooperation area (either from the mainstream or from the on-ramp) if it is assigned a putative leader by the upper level controller (Fig. 3); hence we may have many pairs of successive vehicles, where each vehicle

may act as a follower of its putative and physical leaders; and at the same time be the putative (or physical) leader of other vehicles.

In this context, the scope of this work is, for any given MS, to provide merging trajectories for each involved vehicle, which are traffic-efficient and resolve the merging conflicts as smoothly as possible and with as small engine effort as possible.

3. Vehicle merging trajectory planning

3.1. Trajectory boundary values

The merging trajectory is aimed to guide the vehicle movement from its current state (position and speed) to the merging point, which corresponds to the vehicle's final merging position (Fig. 3). There is a question, however, on how to specify appropriately the final (merging) time and the final (merging) speed for each merging vehicle. Clearly, the difference of the final merging times and speeds of consecutive vehicles are directly related to the time-headway between consecutive exiting vehicles; hence, the specified merging times and speeds of the vehicles will determine the resulting total outflow, or, more generally, the traffic state downstream of the merge. In many circumstances, the mainstream outflow should be maximized, e.g. at times of high demand; more generally, the traffic state downstream of the merge should be optimized according to the prevailing link or network traffic conditions. This is the task of a superior traffic management layer, see e.g. (Roncoli et al., 2015a, 2015b). Thus, there is a necessity for the merging control problem and approach to be conceived in a way that allows for both autonomous operation (in absence of a traffic management layer) and for interventions by a superior traffic management layer, so as to adapt to the prevailing traffic conditions at the link or network level. For the merging control problem at hand, this boils down to an appropriate specification of the final merging times and speeds of merging vehicles, as explained in what follows.

If there is no intervention by an external traffic management level, we will specify (although other choices are also possible within the present framework) that the merging trajectory of each controlled vehicle should, at the final merging point, feature a (final) speed equal to the final speed of its putative leader; and a final time-headway to its leader equal to the prespecified one (set by the driver of the merging vehicle on the on-board (C)ACC system) (Fig. 4). The implication of this choice is that the speed of merging vehicles will be maintained close to the speed of the last merged vehicle which did not have a putative leader or close to the prevailing speed downstream of the merge; while the time-headways of merging vehicles will be the ones set by their drivers. This is a rather "natural" choice which is deemed to lead to smooth traffic conditions, suppressing the nuisance that merging on-ramp vehicles could generate for the freeway traffic. On the other hand, when traffic conditions become critical, the superior traffic management level may be activated and set the final vehicle merging speeds and headways externally, so as to adapt to the prevailing traffic conditions and achieve an efficient traffic flow at link or network level (Fig. 2), as envisaged, e.g. in Kesting et al. (2008) and Roncoli et al. (2015a, 2015b).

When the merging trajectory of the ego vehicle is computed (and continuously updated in real time), its putative leader may not have reached the merging point yet. However, based on the putative leader's own computations, an estimated final merging time and speed is available, which can be communicated to the ego vehicle through V2V or V2I communication (Fig. 2). Thus, the desired final speed v_e of the ego vehicle at the merging point can be estimated (and continuously updated). Moreover, the expected time of arrival T of the ego vehicle at the merging point x_e can be easily computed as

$$T = t_L \tag{1}$$

where t_L is the time that the putative leader is expected to arrive at the position

$$x_T = x_e + v_e \cdot h_d \tag{2}$$

with h_d being the desired headway setting of the ego vehicle. Thus, the ego vehicle should start from the initial condition $\boldsymbol{x_0} = [x_0\ v_0]^T$ and drive to the final condition $\boldsymbol{x_e} = [x_e\ v_e]^T$ by time T at the merging point $x_e = 0$.

The computation and application of an optimal merging trajectory is subject to a variety of potential uncertainties, including: (i) the boundary values t_L and v_e may change over time; (ii) the ACC controller of the ego vehicle may be activated and alter the merging trajectory; (iii) the vehicle's actual path may deviate from the computed merging trajectory; and (iv) as the MS may be modified during the process, a new putative leader may be assigned to the ego vehicle. These uncertainties

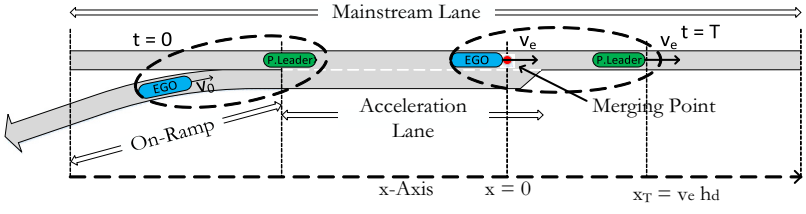

Fig. 4. The positions of the ego vehicle and its putative leader at the beginning and the end of the merging procedure.

call for a feedback control structure to attenuate their impact. We will indeed address this need in later sections of the paper by employing a model predictive control (MPC) approach; i.e. by computing the merging trajectory repeatedly, each time with updated data, during the merging process. Thus, for the needs of this section, we will consider that the boundary values t_L and v_e are available when computing the vehicle merging trajectory.

3.2. Minimization of acceleration

First we will consider the case of defining the optimal merging trajectory as the one that minimizes the required acceleration of each merging vehicle, as .e.g., in Rios-Torres et al. (2015). We consider that the movement of the vehicle is described by the equations of motion and we ignore any delays, lags or restrictions. The system is described by the following state variables:

- $\dot{x}_1 = x_2$ (speed).
- $\dot{x}_2 = u$ (acceleration).

The objective is to bring the system from the initial condition $\boldsymbol{x_0} = [x_0\ v_0]^{\mathrm{T}}$ to the final condition $\boldsymbol{x_e} = [x_e\ v_e]^{\mathrm{T}}$ by time T, while minimizing the criterion

$$J = \frac{1}{2}\int_0^T u^2 dt. \tag{3}$$

This quadratic criterion will lead to smooth variations of acceleration over time. For the sake of simplicity in the form of the optimal solution, we do not consider constraints in the state and control variables. Such constraints would limit the speed between zero and its maximum value; and the acceleration between its minimum and maximum values. Although the probability of actually hitting these bounds in ordinary situations is deemed low, we would in most cases merely face an additional disturbance, should this indeed happen, thanks to the MPC procedure. It should be noted that the derivation of analytical solutions for the corresponding constrained optimization problem is not an easy task and may indeed be even infeasible or computationally demanding due to many possible combinations of subsequent constraint activation and deactivation that would need to be elaborated. In any case, we also offer a (non-analytic) computation possibility with explicit constraint consideration in Section 4.4.

In order to find the solution to the optimal control problem above, we first write its Hamiltonian function

$$H = \frac{1}{2}u^2 + \lambda_1 x_2 + \lambda_2 u \tag{4}$$

where λ_1 and λ_2 are the co-state variables. The necessary conditions for optimality are (Papageorgiou et al., 2012):

$$\dot{x}_1 = H_{\lambda_1} = x_2 \tag{5}$$

$$\dot{x}_2 = H_{\lambda_2} = u \tag{6}$$

$$\dot{\lambda}_1 = -H_{x_1} = 0 \tag{7}$$

$$\dot{\lambda}_2 = -H_{x_2} = -\lambda_1 \tag{8}$$

$$H_u = u + \lambda_2 = 0. \tag{9}$$

From (7) we obtain that

$$\lambda_1(t) = c_1. \tag{10}$$

Hence, from (8) and (9) we have

$$\lambda_2(t) = -c_1 t - c_2 \tag{11}$$

and

$$u(t) = c_1 t + c_2 \tag{12}$$

where c_1 and c_2 are constants to be computed. Using (12), Eqs. (5) and (6) yield:

$$x_1(t) = \frac{1}{6}c_1 t^3 + \frac{1}{2}c_2 t^2 + c_3 t + c_4 \tag{13}$$

$$x_2(t) = \frac{1}{2}c_1 t^2 + c_2 t + c_3. \tag{14}$$

In order to calculate the four constants in (13) and (14), the initial and final conditions of the problem will be used: $x_1(0) = x_0$, $x_1(T) = 0$, $x_2(0) = v_0$, $x_2(T) = v_e$. Then, the corresponding constants result as:

$$c_1 = \frac{6}{T^2}(v_e + v_0) + \frac{12x_0}{T^3} \tag{15}$$

$$c_2 = -\frac{6x_0}{T^2} - \frac{2v_e + 4v_0}{T} \tag{16}$$

$$c_3 = v_0 \tag{17}$$

$$c_4 = x_0. \tag{18}$$

An example demonstrates the performance of the derived optimal solution. Setting $x_0 = -150$ m, $x_e = 0$ m, $v_0 = 14$ $\frac{\text{m}}{\text{s}}$, $v_e = 20$ $\frac{\text{m}}{\text{s}}$, $T = 10$ s, the resulting graphs of jerk (the time derivative of acceleration), acceleration, speed, and position of the merging vehicle as functions of time are presented in Fig. 5.

It is evident that the target speed v_e and target position x_e are achieved at time T as requested; while the acceleration is a linear function of time (see (12)), and the jerk has a small constant value. These trajectories look very smooth at first view. However, it should be emphasized that, using this optimal control formulation, it is impossible to impose an initial acceleration condition. This can be observed in the example, where the optimal solution imposes a certain value of acceleration at time $t = 0^+$, regardless of its actual value (that the merging vehicle had) at time $t = 0^-$. The same can be also observed for the jerk. Since one of our optimization targets is to maximize the passenger comfort, expressed through the minimization of the magnitude and the variation of acceleration, it is necessary to avoid abrupt changes to both acceleration and jerk. This cannot be accomplished by this solution, which, if used within a model predictive control (MPC) framework (as it will be presented in a following section), would result in "step-like" variations in acceleration and corresponding strong pulses in jerk for each discrete time step of the MPC procedure. Similarly, after arrival of the vehicle at the merging point, its speed on the mainstream would be maintained constant at v_e, which implies a jump of acceleration to zero and hence a strong pulse of the jerk value at time T. To circumvent these shortcomings, the problem formulation will be expanded gradually in the next sections.

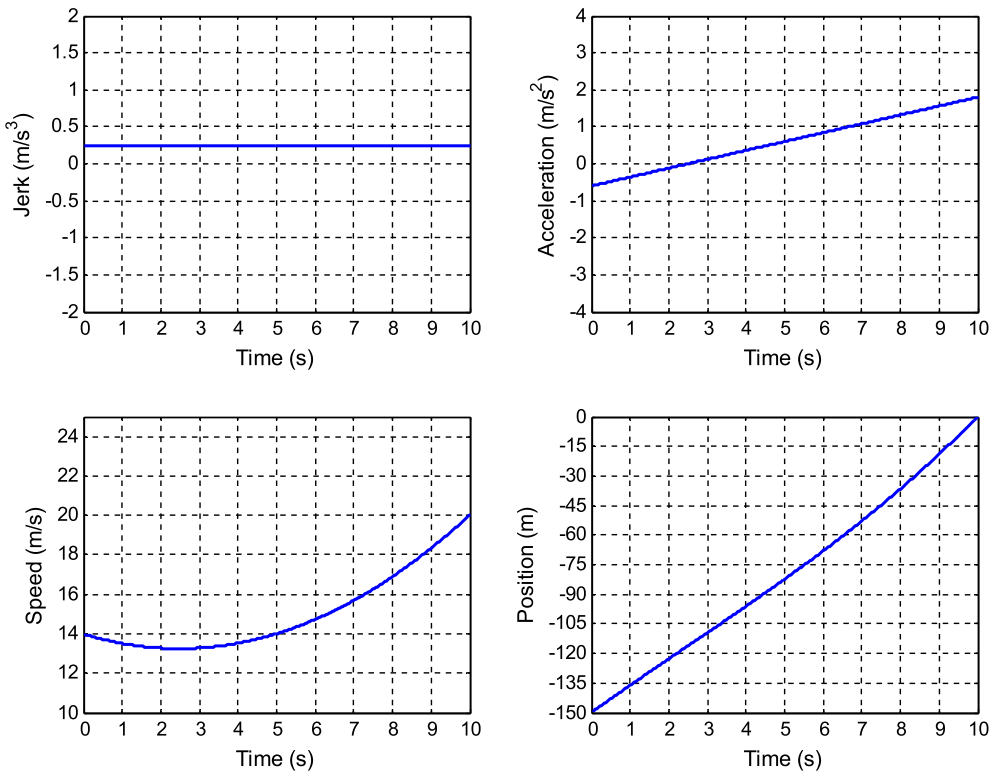

Fig. 5. Graphical representation of the optimal solution, regarding the minimization of acceleration, for the case with $x_0 = -150$ m, $x_e = 0$ m, $v_0 = 14$ $\frac{\text{m}}{\text{s}}$, $v_e = 20$ $\frac{\text{m}}{\text{s}}$, $T = 10$ s.

3.3. Minimization of jerk

We expand the previous formulation so that the acceleration becomes a 3rd state variable while the (virtual) control variable now corresponds to the jerk (the time-derivative of acceleration):

- $\dot{x}_1 = x_2$ (speed).
- $\dot{x}_2 = x_3$ (acceleration).
- $\dot{x}_3 = u$ (jerk).

The objective is to bring the system from the initial condition $\boldsymbol{x_0} = [x_0\ v_0\ a_0]^T$ to the final condition $\boldsymbol{x_e} = [x_e\ v_e\ a_e]^T$ by time T (where a_0 and a_e are the initial and final accelerations of the merging vehicle, respectively), while minimizing the criterion:

$$J = \frac{1}{2}\int_0^T u^2 dt. \tag{19}$$

The Hamiltonian function of the above optimal control problem is

$$H = \frac{1}{2}u^2 + \lambda_1 x_2 + \lambda_2 x_3 + \lambda_3 u \tag{20}$$

where λ_1, λ_2, λ_3,are the co-state variables. Subsequently, we have the necessary conditions of optimality:

$$\dot{x}_1 = H_{\lambda_1} = x_2 \tag{21}$$

$$\dot{x}_2 = H_{\lambda_2} = x_3 \tag{22}$$

$$\dot{x}_3 = H_{\lambda_3} = u \tag{23}$$

$$\dot{\lambda}_1 = -H_{x_1} = 0 \tag{24}$$

$$\dot{\lambda}_2 = -H_{x_2} = -\lambda_1 \tag{25}$$

$$\dot{\lambda}_3 = -H_{x_3} = -\lambda_2 \tag{26}$$

$$H_u = u + \lambda_3 = 0. \tag{27}$$

By solving (24), we obtain again (10); and using (25), we get again (11). Using (26), we then have

$$\lambda_3(t) = \frac{1}{2}c_1 t^2 + c_2 t + c_3. \tag{28}$$

Finally, due to (27) we have:

$$u(t) = -\lambda_3(t) = -\frac{1}{2}c_1 t^2 - c_2 t - c_3 \tag{29}$$

$$x_3(t) = -\frac{1}{6}c_1 t^3 - \frac{1}{2}c_2 t^2 - c_3 t - c_4 \tag{30}$$

$$x_2(t) = -\frac{1}{24}c_1 t^4 - \frac{1}{6}c_2 t^3 - \frac{1}{2}c_3 t^2 - c_4 t - c_5 \tag{31}$$

$$x_1(t) = -\frac{1}{120}c_1 t^5 - \frac{1}{24}c_2 t^4 - \frac{1}{6}c_3 t^3 - \frac{1}{2}c_4 t^2 - c_5 t - c_6. \tag{32}$$

In this case, six constants have to be specified for the 5th order polynomial of (32), using the initial and final conditions of the involved state variables. The conditions used for the previous formulation (for position and speed) are maintained. In addition, we specify that: (a) the initial acceleration equals the actual acceleration a_0 of the merging vehicle at time zero (to avoid jumps of the acceleration value with MPC); and (b) the final acceleration should be equal to zero (to avoid an acceleration jump at the merging point). Hence, the six conditions can be formulated as: $x_1(0) = x_0$, $x_1(T) = 0$, $x_2(0) = v_0$, $x_2(T) = v_e$, $x_3(0) = a_0$, $x_3(T) = 0$. These conditions lead to an analytic calculation of the six constants, as detailed in Appendix A.

The example demonstrates the performance of the derived optimal solution. The initial and final conditions are: $x_0 = -150$ m, $x_e = 0$ m, $v_0 = 14\ \frac{\text{m}}{\text{s}}$, $v_e = 20\ \frac{\text{m}}{\text{s}}$, $a_0 = -0.6\ \frac{\text{m}}{\text{s}^2}$, $a_e = 0.0\ \frac{\text{m}}{\text{s}^2}$, $T = 10$ s. Note that the initial value of acceleration is chosen equal to the same value in the previous example, to enable comparability of results.

The graphical representation of the resulting optimal solutions is depicted in Fig. 6. It can be observed that the derived optimal solution provides the expected results concerning the initial and final conditions. The jerk is seen to exhibit some

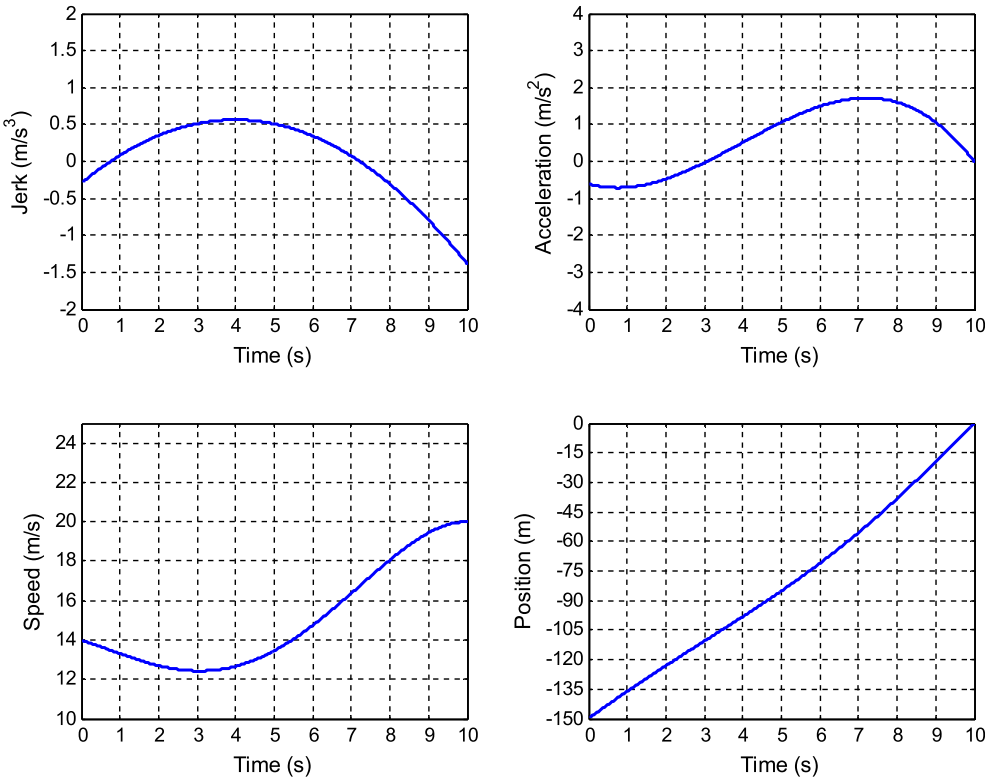

Fig. 6. Graphical representation of the optimal solution, regarding the minimization of jerk, for the case with $x_0 = -150$ m, $x_e = 0$ m, $v_0 = 14\ \frac{\text{m}}{\text{s}}$, $v_e = 20\ \frac{\text{m}}{\text{s}}$, $a_0 = -0.6\ \frac{\text{m}}{\text{s}^2}$, $a_e = 0.0\ \frac{\text{m}}{\text{s}^2}$, $T = 10$ s.

variations compared to its constant value in Fig. 5; which is the price to pay in order to impose the initial and final acceleration values and hence avoid jerk pulses at the start and final times. However, we still face the problem of jerk jumps at the initial and final states in case of MPC application. Since this may have a direct impact on passenger feeling and comfort, we may address this issue by also taking into account the derivative of the jerk in the state equations.

3.4. Minimization of the derivative of jerk

The system is now described by the following state variables:

- $\dot{x}_1 = x_2$ (speed).
- $\dot{x}_2 = x_3$ (acceleration).
- $\dot{x}_3 = x_4$ (jerk).
- $\dot{x}_4 = u$ (derivative of jerk).

The objective is to bring the system from the initial condition $\boldsymbol{x_0} = [x_0\ v_0\ a_0\ j_0]^{\text{T}}$ to the final condition $\boldsymbol{x_e} = [x_e\ v_e\ a_e\ j_e]^{\text{T}}$ by time T (where j_0 and j_e are the initial and final values of jerk for the merging vehicle, respectively), while minimizing the criterion:

$$J = \frac{1}{2}\int_0^T u^2 dt. \tag{33}$$

The Hamiltonian function of the above optimal control problem is now

$$H = \frac{1}{2}u^2 + \lambda_1 x_2 + \lambda_2 x_3 + \lambda_3 x_4 + \lambda_4 u \tag{34}$$

where λ_1, λ_2, λ_3, λ_4, are the co-state variables. Following the same procedure as before, the optimal solution is given by:

$$u = (c_1 t^3/6) + (c_2 t^2/2) + c_3 t + c_4. \tag{35}$$

Subsequently,

$$x_4 = \frac{c_1 t^4}{24} + \frac{c_2 t^3}{6} + \frac{c_3 t^2}{2} + c_4 t + c_5 \tag{36}$$

$$x_3 = \frac{c_1 t^5}{120} + \frac{c_2 t^4}{24} + \frac{c_3 t^3}{6} + \frac{c_4 t^2}{2} + c_5 t + c_6 \tag{37}$$

$$x_2 = \frac{c_1 t^6}{720} + \frac{c_2 t^5}{120} + \frac{c_3 t^4}{24} + \frac{c_4 t^3}{6} + \frac{c_5 t^2}{2} + c_6 t + c_7 \tag{38}$$

$$x_1 = \frac{c_1 t^7}{5040} + \frac{c_2 t^6}{720} + \frac{c_3 t^5}{120} + \frac{c_4 t^4}{24} + \frac{c_5 t^3}{6} + \frac{c_6 t^2}{2} + c_7 t + c_8. \tag{39}$$

In this case, eight constants have to be defined for the 7th degree polynomial of Eq. (39), using the initial and final conditions of the problem at hand. The conditions used for the previous formulation are maintained, and the two additional conditions needed are set as follows: (a) the initial jerk equals the actual jerk of the merging vehicle at time zero (to avoid initial jumps) and (b) the final jerk is set zero (for similar reasons as in the previous formulation). The eight conditions can be given now as: $x_1(0) = x_0$, $x_1(T) = 0$, $x_2(0) = v_0$, $x_2(T) = v_e$, $x_3(0) = a_0$, $x_3(T) = 0$, $x_4(0) = j_0$, $x_4(T) = 0$, where j_0 is the initial jerk of the merging vehicle.

The following example demonstrates the performance of the derived optimal solution. The initial and final conditions are: $x_0 = -150$ m, $x_e = 0$ m, $v_0 = 14$ $\frac{\text{m}}{\text{s}}$, $v_e = 20$ $\frac{\text{m}}{\text{s}}$, $a_0 = -0.6$ $\frac{\text{m}}{\text{s}^2}$, $a_e = 0.0$ $\frac{\text{m}}{\text{s}^2}$, $j_0 = -0.3$ $\frac{\text{m}}{\text{s}^3}$, $j_e = 0$ $\frac{\text{m}}{\text{s}^3}$, $T = 10$ s. The graphical representation of the resulting optimal solutions is depicted in Fig. 7. As it can be observed, the derived optimal solution provides the expected results, concerning the initial and final conditions. Again, jerk and acceleration are varying with time to ensure the satisfaction of initial and final conditions. Note, in particular, the increasingly smooth convergence of the speed towards its final value over the three cases of Figs. 5–7.

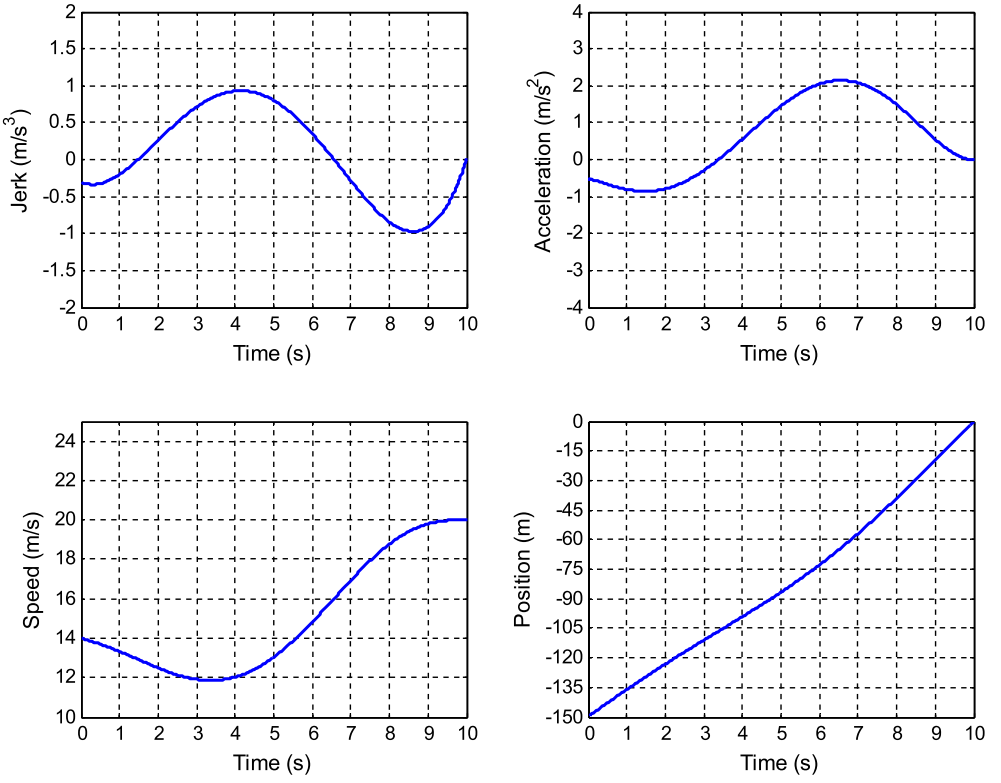

Fig. 7. Graphical representation of the optimal solution, regarding the minimization of the derivative of jerk, for the case with $x_0 = -150$ m, $x_e = 0$ m, $v_0 = 14$ $\frac{\text{m}}{\text{s}}$, $v_e = 20$ $\frac{\text{m}}{\text{s}}$, $a_0 = -0.6$ $\frac{\text{m}}{\text{s}^2}$, $a_e = 0.0$ $\frac{\text{m}}{\text{s}^2}$, $j_0 = -0.3$ $\frac{\text{m}}{\text{s}^3}$, $j_e = 0$ $\frac{\text{m}}{\text{s}^3}$, $T = 10$ s.

4. Further extensions

4.1. Combined cost function

In the previous section, the considered cost function includes only the (virtual) control input u. This, however, may not provide sufficient flexibility while attempting an appropriate, possibly individual (by driver) trade-off between engine effort, passenger comfort and task feasibility. The generalization in this section considers a combined cost function, taking into account the acceleration, the jerk, as well as the time-derivative of jerk. To this end, a weighted sum of the respective terms is used to define the new cost function. The first two terms in the combined cost function are directly related to comfort and engine effort, respectively. On the other hand, the derivative of jerk does not have a direct physical meaning; however, it is necessary to include it in the cost function for avoiding abrupt jerk changes at the start and end of the merging maneuver. The system is described with four state equations, as in Section 3.4., and the objective is to bring the system from the condition $\boldsymbol{x_0} = [x_0\ v_0\ a_0\ j_0]^{\mathrm{T}}$ to the final condition $\boldsymbol{x_e} = [0\ v_e\ 0\ 0]^{\mathrm{T}}$ by time T.

The cost function is now defined as:

$$J = \frac{1}{2}\int_0^T (w_1 x_3^2 + w_2 x_4^2 + u^2)dt \tag{40}$$

where w_1, w_2 are the non-negative weights of the two additional terms in the cost function. The Hamiltonian function of the optimal control problem above is

$$H = \frac{1}{2}(w_1 x_3^2 + w_2 x_4^2 + u^2) + \lambda_1 x_2 + \lambda_2 x_3 + \lambda_3 x_4 + \lambda_4 u \tag{41}$$

where λ_1, λ_2, λ_3, λ_4 are the co-state variables. Following a similar procedure as before, the optimal solution results as:

$$u(t) = c_5 \cdot A_1^4 \cdot e^{A_1 * t} + c_6 \cdot A_1^4 \cdot e^{-A_1 * t} + c_7 \cdot A_2^4 \cdot e^{A_2 * t} + c_8 \cdot A_2^4 \cdot e^{-A_2 * t} \tag{42}$$

$$x_4 = \frac{c_1}{w_1} + c_5 \cdot A_1^3 \cdot e^{A_1 * t} - c_6 \cdot A_1^3 \cdot e^{-A_1 * t} + c_7 \cdot A_2^3 \cdot e^{A_2 * t} - c_8 \cdot A_2^3 \cdot e^{-A_2 * t} \tag{43}$$

$$x_3 = \frac{c_2}{w_1} + \frac{c_1}{w_1} t + c_5 \cdot A_1^2 \cdot e^{A_1 * t} + c_6 \cdot A_1^2 \cdot e^{-A_1 * t} + c_7 \cdot A_2^2 \cdot e^{A_2 * t} + c_8 \cdot A_2^2 \cdot e^{-A_2 * t} \tag{44}$$

$$x_2 = \frac{c_3}{w_1} + \frac{c_2}{w_1} t + \frac{c_1 w_2}{w_1^2} + \frac{c_1}{2w_1} t^2 + c_5 \cdot A_1 \cdot e^{A_1 * t} - c_6 \cdot A_1 \cdot e^{-A_1 * t} + c_7 \cdot A_2 \cdot e^{A_2 * t} - c_8 \cdot A_2 \cdot e^{-A_2 * t} \tag{45}$$

$$x_1 = \frac{w_2 c_1}{w_1^2} t + \frac{w_2 c_2}{w_1^2} + \frac{c_1}{6w_1} t^3 + \frac{c_2}{2w_1} t^2 + \frac{c_3}{w_1} t + \frac{c_4}{w_1} + c_5 \cdot e^{A_1 * t} + c_6 \cdot e^{-A_1 * t} + c_7 \cdot e^{A_2 * t} + c_8 \cdot e^{-A_2 * t} \tag{46}$$

where

$$A_1 = \sqrt{\frac{w_2 - \sqrt{w_2^2 - 4w_1}}{2}} \tag{47}$$

$$A_2 = \sqrt{\frac{w_2 + \sqrt{w_2^2 - 4w_1}}{2}}. \tag{48}$$

It should be noted that the above solution is valid only if $w_2^2 - 4w_1 \neq 0$. Otherwise, the optimal solution is given by:

$$x_1 = \frac{w_2 c_1}{w_1^2} t + \frac{w_2 c_2}{w_1^2} + \frac{c_1}{6w_1} t^3 + \frac{c_2}{2w_1} t^2 + \frac{c_3}{w_1} t + \frac{c_4}{w_1} + c_5 \cdot e^{\sqrt{\frac{w_2}{2}} * t} + c_6 \cdot e^{-\sqrt{\frac{w_2}{2}} * t} + c_7 \cdot t \cdot e^{\sqrt{\frac{w_2}{2}} * t} + c_8 \cdot t \cdot e^{-\sqrt{\frac{w_2}{2}} * t}. \tag{49}$$

The eight conditions for the computation of the eight constants in (49) are the same as in Section 3.4: $x_1(0) = x_0, x_1(T) = 0$, $x_2(0) = v_0$, $x_2(T) = v_e$, $x_3(0) = a_0$, $x_3(T) = 0$, $x_4(0) = j_0$, $x_4(T) = 0$. This solution will be used to investigate the impact of the cost function weights in a later section. It should be emphasized that all optimal control solutions obtained to this point can be readily executed in real time (within a MPC framework) in the vehicle's on-board computer, as they only require elementary computations and the inversion of a low-order matrix (see Appendix A).

4.2. Discrete-time formulation

The previous optimal control problems may also be formulated in discrete time, in which case the resulting optimization may be cast in the form of a Quadratic Programming (QP) problem (Papageorgiou et al., 2012). Let τ be the discrete time step.

Let $a_k = a(k\tau), j_k = j(k\tau), d_k = d(k\tau)$ be the acceleration, the jerk and the time derivative of jerk, respectively, at discrete time instant $k = 0, 1, 2, \ldots K$, with $K = T/\tau$ being the total number of discrete time steps. Then the cost function to be minimized is

$$Z = \sum_{k=0}^{K-1} \left(w_1 a_k^2 + w_2 j_k^2 + d_k^2 \right). \tag{50}$$

Similarly, we define with x_k and v_k the position and speed of the vehicle at time instant k. Assuming a constant value of the (virtual) control variable d_k during each time step $[k\tau,(k+1)\tau)$, the state variables should obey the following linear discrete-time state equations:

$$x_{k+1} = x_k + v_k\tau + \frac{1}{2}a_k\tau^2 + \frac{1}{6}j_k\tau^3 + \frac{1}{24}d_k\tau^4 \tag{51}$$

$$v_{k+1} = v_k + a_k\tau + \frac{1}{2}j_k\tau^2 + \frac{1}{6}d_k\tau^3 \tag{52}$$

$$a_{k+1} = a_k + j_k\tau + \frac{1}{2}d_k\tau^2 \tag{53}$$

$$j_{k+1} = j_k + d_k\tau \tag{54}$$

with the following initial and final conditions:

$$\begin{aligned} &x_0 = x(0), \quad x_K = x(K) = 0 \\ &v_0 = v(0), \quad v_K = v(K) \\ &a_0 = a(0), \quad a_K = a(K) = 0 \\ &j_0 = j(0), \quad j_K = j(K) = 0. \end{aligned} \tag{55}$$

The only difference of this discrete-time optimal control problem from its continuous-time counterpart of Section 4.1 is due to the fact that the (virtual) control variable d_k is constant for the duration of each time period τ. Hence, the solution of both problems will be virtually identical for sufficiently small τ. In fact, solving the discrete-time problem with $\tau = 0.01$ s was found to produce virtually indistinguishable solutions when compared with the continuous-time solutions; but much larger time steps may be sufficient for practice-relevant results. Despite the impressive recent advancements with solution codes for QP control problems (Mattingley et al., 2011), the formulation of the merging trajectory design problem in QP format is not expected to provide computational advantages over the reported solutions of Sections 3 and 4.1. However, the QP formulation would allow for ready inclusion (if necessary) of linear state or control constraints, as described in Section 4.4.

4.3. The choice of weights

In the case of minimization of the combined cost function, which includes two weighted terms, the choice of weights plays an important role for the shape of the resulting optimal trajectories. In particular, possible extreme values of jerk and acceleration can be suppressed by the proper selection of weights. Undoubtedly, some drivers may be skeptical regarding the produced optimal merging trajectories, especially if they do not match their driving preferences; this might in turn lead to deactivation of the system. However, the use of weights in the formulation of the problem as tuning parameters could possibly render the system more appealing to the drivers, if the weights could be manually adjusted by the individual driver to render the resulting trajectories more appealing to her driving style. An alternative option would be to use machine learning techniques to automatically tune these weights, using as a learning base the trajectories the specific driver usually applies for merging.

To illustrate the impact each weight has on the produced optimal trajectory, a range of different examples is presented. The initial and final conditions for all considered examples are the same as in Section 3.4. In the first case considered, the weight w_2 is kept constant ($w_2 = 1$), while varying the weight w_1. In the second case, the weight w_1 is kept constant ($w_1 = 1$), while varying the weight w_2. In the third case, both weights vary, having the same value for each sub-case. The corresponding results are depicted in Figs. 8–10. The variation of only w_2 (Fig. 9) seems to have a small effect on the time variation of acceleration and jerk, while the variation of only w_1 (Fig. 8) has the more pronounced effect. As w_1 is increasing, the tendency to minimize the acceleration becomes higher and leads to a linear-like trajectory (as in Section 3.2), but the zero-acceleration constraint at the final time produces an abrupt variation in acceleration and correspondingly high values of jerk, near the end of the trajectory. When both weights are modified (with equal values, to demonstrate the effect of the third term of the cost function, see Fig. 10), the variation of jerk is higher for the large values of both weights due to the combined effect of the two first terms of the cost function; while, for small values of the two weights, the variation of acceleration and jerk is rather small. Clearly a high number of different merging examples, involving various initial and final states as well as final times, may be necessary to appreciate the impact of weights and the related possibilities.

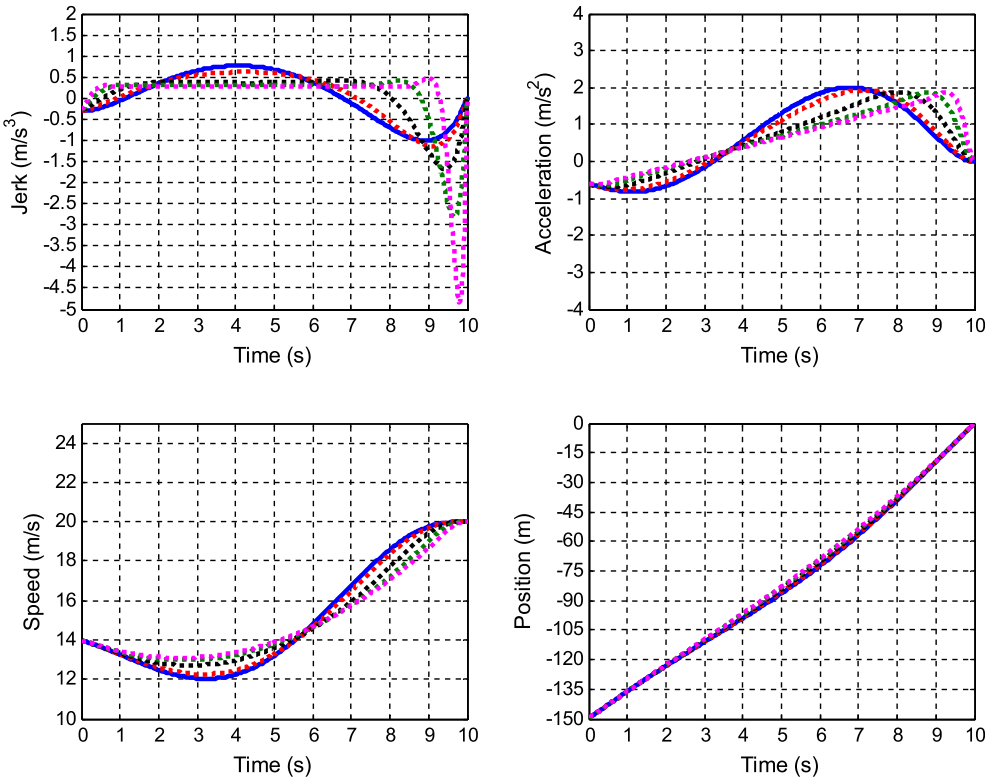

Fig. 8. Graphical representation of the resulting optimal solutions, regarding the minimization of the combined cost function, for different values of w_1; $w_2 = 1$, $w_1 = 0.1$ (*blue*), 1 (*red*), 10 (*black*), 100 (*green*), 1000 (*magenta*). (For interpretation of the references to colour in this figure legend, the reader is referred to the web version of this article.)

4.4. QP formulation with inequality constraints

The QP formulation can be used to compute the optimal solution in the case where constraints are also imposed for the maximum and minimum permissible values of the state variables. This is demonstrated in the following example, referring to the case with the combined cost function, with the same initial and final conditions and the weights $w_1 = 0.1$, $w_2 = 0.5$. The optimal solution for the unconstrained case is visible in Fig. 11, along with the resulting optimal solution when a maximum value in acceleration equal to $a_{max} = 1.5\ \frac{\mathrm{m}}{\mathrm{s}^2}$ is imposed. The optimal solution is accordingly modified to satisfy the imposed constraint, resulting in steeper variations of jerk outside the region where the constraint is activated, in order to fulfil the initial and final conditions.

4.5. Time-varying LQR (Linear-Quadratic Regulator) formulation

The unconstrained optimal control problem (for the continuous-time or the discrete-time formulation) is a Linear Quadratic (LQ) one, since the system state is described by a set of linear differential or difference equations, while the cost function is of quadratic form. Thus, the solution of this problem can be given in linear feedback form, as a linear-quadratic-regulator (LQR). The LQR may be developed in very similar ways in either continuous time or discrete time. In the following the discrete-time LQR derivation is presented for the problem under consideration.

Eqs. (51)–(54) constitute a discrete-time linear system which may be expressed in state-space form

$$\boldsymbol{x}_{k+1} = \boldsymbol{A} \cdot \boldsymbol{x}_k + \boldsymbol{b} \cdot u_k \tag{56}$$

where $\boldsymbol{x} = [x\ v\ a\ j]^{\mathrm{T}}$ is the state vector and $u = d$ is the (virtual) control input. The quadratic performance index (50) is extended with a final-time term

$$J = \frac{1}{2}\|\boldsymbol{x}_K\|_{\boldsymbol{S}}^2 + \frac{1}{2}\sum_{k=0}^{K-1}\left[\|\boldsymbol{x}_k\|_{\boldsymbol{Q}}^2 + u_k^2\right]. \tag{57}$$

As in (50), we have the diagonal state-weighting matrix $\boldsymbol{Q} = diag(0\ 0\ w_1\ w_2)$. The final-time term is introduced to guarantee that all final states $\boldsymbol{x}_K$ will be virtually zero; to this end, the elements of the diagonal weighting matrix $\boldsymbol{S}$ are chosen sufficiently high.

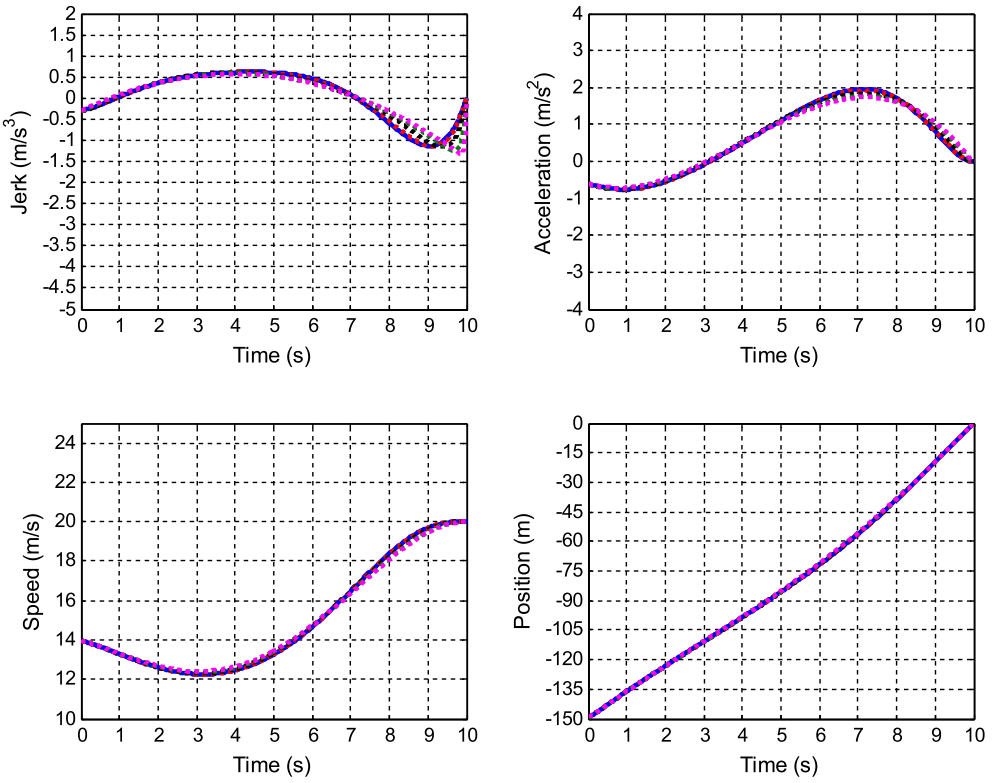

Fig. 9. Graphical representation of the resulting optimal solutions, regarding the minimization of the combined cost function, for different values of w_2; $w_1 = 1$, $w_2 = 0.1$ (*blue*), 1 (*red*), 10 (*black*), 100 (*green*), 1000 (*magenta*). (For interpretation of the references to colour in this figure legend, the reader is referred to the web version of this article.)

It can be shown (Papageorgiou et al., 2012) that the optimal control sequence minimizing the performance index is delivered by the linear feedback law

$$u_k = -\boldsymbol{L}_k \cdot \boldsymbol{x}_k \tag{58}$$

where $\boldsymbol{L}$ is the time-varying feedback gain vector, which may be computed via the following equations

$$\boldsymbol{L}_k = \left[\boldsymbol{b}^{\mathrm{T}}\boldsymbol{P}_{k+1}\boldsymbol{b} + 1\right]^{-1}\left[\boldsymbol{b}^{\mathrm{T}}\boldsymbol{P}_k\boldsymbol{A}\right] \tag{59}$$

$$\boldsymbol{P}_k = \boldsymbol{A}^{\mathrm{T}}\boldsymbol{P}_{k+1}\boldsymbol{A} + \boldsymbol{Q} - \boldsymbol{L}_k^{\mathrm{T}}\boldsymbol{b}^{\mathrm{T}}\boldsymbol{P}_{k+1}\boldsymbol{A} \tag{60}$$

with terminal condition

$$\boldsymbol{P}_K = \boldsymbol{S}. \tag{61}$$

The matrix $\boldsymbol{P}_k$ is referred to as the discrete-time Riccati matrix and it can be computed, along with the gain $\boldsymbol{L}_k$, through backward integration, starting from (61) and utilizing Eqs. (59) and (60).

The above feedback control law will drive the system to the origin ($\boldsymbol{x}_K = 0$) in final time K from any initial state $\boldsymbol{x}(0) = \boldsymbol{x}_0$. In our case however, we need all final states to be driven to the origin, except for the speed, which should be driven towards the desired final speed v_e. For this reason, the problem must be reformulated such that all states are driven to zero. To this end, we introduce the variable v^* as

$$v_k^* = v_k - v_e. \tag{62}$$

Eq. (51) for the position now becomes

$$x_{k+1} = x_k + v_k^*\tau + \frac{1}{2}a_k\tau^2 + \frac{1}{6}j_k\tau^3 + \frac{1}{24}d_k\tau^4 + v_e\tau. \tag{63}$$

Accordingly, Eq. (52) for the speed becomes

$$v_{k+1}^* = v_k^* + a_k\tau + \frac{1}{2}j_k\tau^2 + \frac{1}{6}d_k\tau^3. \tag{64}$$

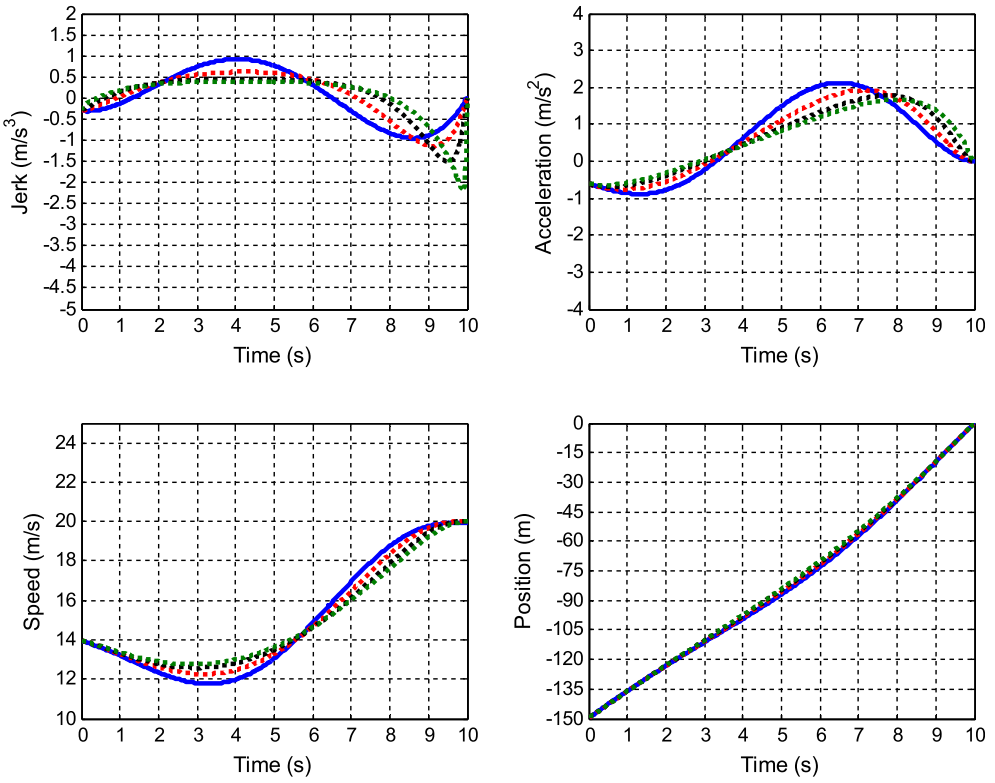

Fig. 10. Graphical representation of the resulting optimal solutions, regarding the minimization of the combined cost function, for different values of $w_1 = w_2$; $w_1 = w_2 = 0.0001$ (*blue*), 1 (*red*), 10 (*black*), 1000 (*green*). (For interpretation of the references to colour in this figure legend, the reader is referred to the web version of this article.)

The remaining system equations (acceleration and jerk) remain unchanged. The new equations may be written in state-space form

$$\boldsymbol{x}_{k+1} = \boldsymbol{A} \cdot \boldsymbol{x}_k + \boldsymbol{b} \cdot u_k + \boldsymbol{\delta} \tag{65}$$

where now $\boldsymbol{x} = [x\ v^* a\ j]^{\mathrm{T}}$ and the vector $\boldsymbol{\delta} = [v_e\ \tau\ 0\ 0\ 0]^{\mathrm{T}}$ acts as a constant and known disturbance to the system. In this case, the optimal control law is extended (Marinaki and Papageorgiou, 2005) as

$$u_k = -\boldsymbol{L}_k \boldsymbol{x}_k - U_k \tag{66}$$

For computing the feedforward term U_k, we use the following definitions:

$$\boldsymbol{D}_k = [1 + \boldsymbol{b}^{\mathrm{T}} \boldsymbol{P}_{k+1} \boldsymbol{b}]^{-1} \boldsymbol{b}^T \tag{67}$$

$$\boldsymbol{Z}_k = \boldsymbol{A}^{\mathrm{T}} [\boldsymbol{I} - \boldsymbol{P}_{k+1} \boldsymbol{b} \boldsymbol{D}_k] \tag{68}$$

$$\boldsymbol{p}_K = \boldsymbol{P}_K \boldsymbol{\delta} \tag{69}$$

$$\boldsymbol{p}_k = \boldsymbol{P}_k \boldsymbol{\delta} + \boldsymbol{Z}_k \boldsymbol{p}_{k+1} \tag{70}$$

The vector $\boldsymbol{p}_k$ can be computed using Eqs. (67)–(70). Finally we have $U_k = \boldsymbol{D}_k \boldsymbol{p}_{k+1}$.

It is important to note that the matrices $\boldsymbol{P}_k$ and $\boldsymbol{L}_k$ can be computed offline only once, for a sufficiently long K, and be stored inside the vehicle, since they depend only on the a priori known matrices $\boldsymbol{A}, \boldsymbol{b}, \boldsymbol{Q}$; while the feedforward term U_k depends also on the desired final speed (v_e) and must therefore be computed online (or be stored for a range of different final speeds).

The LQR solution is equivalent to the previously derived analytical solution, but might present computational advantages. In particular, the control law (66) is by itself equivalent to an MPC procedure, because it is not dependent on any particular initial state.

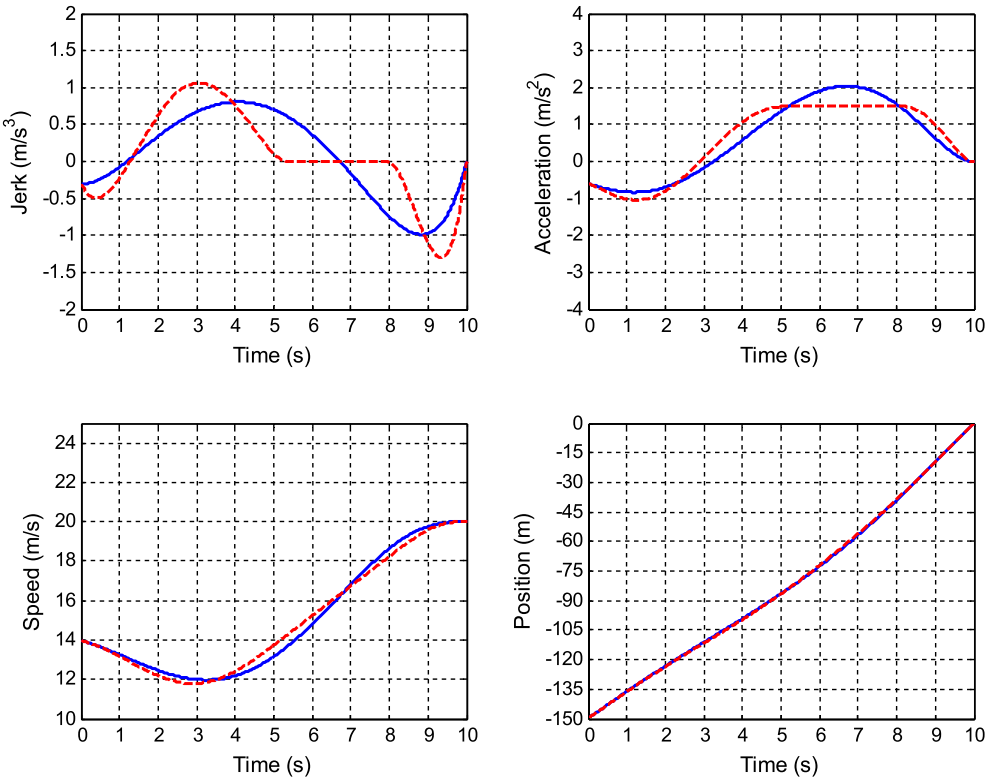

Fig. 11. Graphical representation of the resulting optimal solutions using QP, regarding the minimization of the combined cost function, for the case with $x_0 = -150$ m, $x_e = 0$ m, $v_0 = 14\ \frac{m}{s}$, $v_e = 20\ \frac{m}{s}$, $a_0 = -0.6\ \frac{m}{s^2}$, $a_e = 0\ \frac{m}{s^2}$, $j_0 = -0.3\ \frac{m}{s^3}$, $j_e = 0\ \frac{m}{s^3}$, $T = 10$ s; solid blue line: no constraints are activated; dashed red line: imposed maximum acceleration constraint $a_{max} = 1.5\ \frac{m}{s^2}$. (For interpretation of the references to colour in this figure legend, the reader is referred to the web version of this article.)

4.6. Lateral movement

For the final merging of vehicles stemming from the on-ramp, a lateral lane change from the acceleration lane to the mainstream lane is of course necessary. All previous developments did not address explicitly this lateral part of the on-ramp merging vehicle trajectory. This is because the presence of a fixed merging point (Fig. 1) allows for an independent design of the lateral vehicle movement. Specifically, on-ramp merging vehicles need to move, short before reaching the merging point, in lateral direction from an initial position $y(0) = -\Delta$, Δ being the lane width, to zero. The time period for the execution of the lane change maneuver may be pre-specified to be either constant (few seconds) or dependent on the desired longitudinal merging speed v_e. The initial speed, acceleration and jerk in lateral direction at the start of the maneuver are obviously equal to zero; while the respective final values at the end of the maneuver should also be equal to zero. The state equations and objective criterion for the lateral movement are the same as for the longitudinal movement in previous sections. However, since the final values of all lateral state variables must be equal to zero, the ordinary LQR (58), with offline computed gain matrix, may be employed online for the lateral movement with very low computation requirements.

5. Application of a model predictive control framework

5.1. The necessity of MPC

In the previous sections we adopted the assumption that each merging vehicle knows its final speed (v_e) and time of arrival at the merging point (T) beforehand, while computing its trajectory. However, these values may be subject to modifications as the vehicle is moving in an actual merging scenario for several reasons, such as: (a) inaccurate estimation of the expected speed and time of arrival at the merging point of the previous vehicle in the MS (putative leader); (b) inaccurate trajectory realization by the vehicle control; (c) the presence of other vehicles ahead of the putative leader may affect its trajectory and its time of arrival to the merging point (as well as its expected speed); and (d) changes of the final speed and headway ordered by the traffic management level (Fig. 2).

In order to tackle such real-time changes, which call for corresponding updates of the vehicle trajectory, a Model Predictive Control (MPC) scheme is utilized. In this way, possible disturbances in the trajectories of the merging vehicle and its

putative leader can be compensated, as the optimization problem is repeatedly solved (or the LQR is applied in real time), using the updated data for the formation of the remaining part of the optimal trajectory. Thanks to the pursued problem formulation, the optimal solution's general form remains always the same (in every time step); what changes are only the initial state, the remaining time horizon and, possibly, the final merging speed. Thus, the solution constants can be re-calculated as functions of the initial conditions, as well as of v_e and T; or the LQR (66) may be simply activated, possibly with an update of the feedforward term, in case of final speed change. This procedure is repeated regularly, e.g. each second; until the vehicle merging has been actually accomplished.

In the following section, illustrative MPC-application examples will be presented for cases where unexpected modifications in the movement of the putative leader occur, which affect both T and v_e.

5.2. MPC application examples

We assume in this section that the putative leader can transmit only its current speed and position to the ego vehicle. Therefore, it is necessary to make an assumption regarding the future movement of the putative leader, which will enable the ego vehicle to estimate its expected time of arrival (T) and expected speed (v_e) and be able to apply the optimal control. The simplest assumption for estimating the aforementioned values is the one of constant speed for the remaining part of the trajectory of the putative leader. Clearly, this naïve assumption presents a challenge to the ego vehicle if the leader is actually changing its speed, hence the resulting merging control may, under circumstances, lead to strong (or even extreme) acceleration requirements. Under this assumption, the putative leader will move at constant speed from the current time $t = t_0$ until the time $t = t_0 + T$. Consequently, the expected speed and expected time of arrival of the ego vehicle can be easily calculated as follows:

$$v_e = v_L(t_0) \tag{71}$$

$$T = \left|\frac{h_d \cdot v_e - x_L(t_0)}{v_L(t_0)}\right| = \left|h_d - \frac{x_L(t_0)}{v_L(t_0)}\right| \tag{72}$$

where the subscript "L" refers to the putative leader. If, for any reason, the putative leader is stopped in the current time step (i.e. $v_L(t_0) = 0$), a suitable trajectory is applied to the ego vehicle, so as to have it stop at a safe distance behind the putative leader. In order to calculate this trajectory we set $v_e = 0$, while T is calculated from

$$T = \frac{v}{a_{comf}} \tag{73}$$

where α_{comf} is a comfortable deceleration. Also, since the optimal solutions are designed to satisfy the final condition $x(T) = 0$, the x-axis for this exceptional case should be suitably "shifted"; such that the new initial position to be used in the optimal solution calculation is $x' = x - (x_L - (l_L + r_{safe}))$, where l_L is the length of the putative leader and r_{safe} is the safe distance.

In the first example (Fig. 12), the putative leader drives at a constant speed of 15 m/s; then it accelerates to 20 m/s; and continues thereafter at a constant speed. The ego vehicle assumes, at each MPC update, a constant future speed for its putative leader, equal the leader's current speed. The simulation step is equal to 0.01 s, while $w_1 = 0.1$, $w_2 = 0.5$. In Fig. 12, different results of the MPC scheme are presented for different values of the MPC control step used (control step: blue = 0.1 s, red = 0.5 s, black = 2.0 s).

From Fig. 12 it may be seen that the system works as expected, converging to the prescribed final speed and headway. However, by increasing the control intervals, the total cost is also increasing (Table 1) because, in order to address the accumulated estimation error in cases of longer control steps, the ego vehicle needs to apply stronger maneuvers.

Simulations have been also performed for the case where the leader continues to accelerate throughout the duration of the merging process. This example was introduced to illustrate the difficulties that might arise in case of a naïve MPC prediction regarding the leader's speed. In such a case, there will always be a speed and headway error at the end of the merging maneuver, since the ego vehicle assumes constant leader speed, while the putative leader actually accelerates. Particularly, when the ego vehicle is close to the merging point, the remaining time is not sufficient to compensate for the error, and the optimal solution may impose large accelerations. This situation can be improved if the prediction regarding T and v_e can become more accurate (not using the assumption of constant speed for the remaining of the trajectory), or the putative leader can communicate its estimated final merging time and speed according to its own optimal trajectory planning. In order to visualize this problem, the example in Fig. 13 is used. Note that, if hard inequality constraints (for acceleration and speed) would be considered here, this might render the optimization problem infeasible.

5.3. Comparison with ACC-controller merging

In this section, the proposed method will be compared to a typical ACC controller (Ntousakis et al., 2014b) merging policy. As a matter of fact, several works have proposed the derivation of a merging trajectory for the ego vehicle by applying its ACC control law to a so-called "virtual" vehicle, which is basically a "projection" of the putative leader to the same lane as the ego

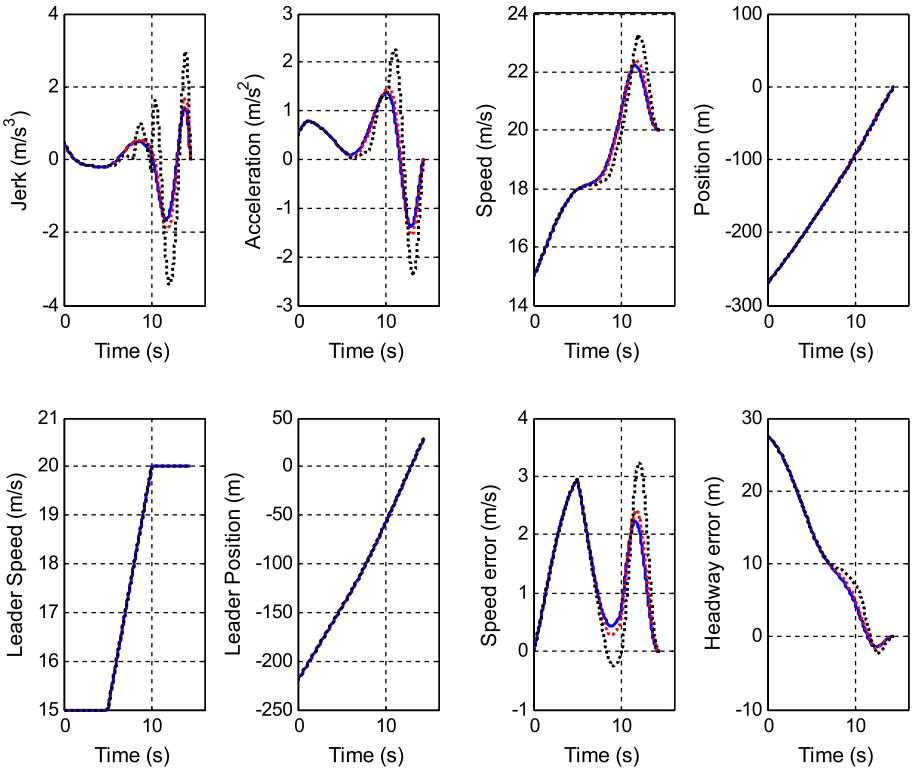

Fig. 12. The effect of the control step on the resulting trajectory with the MPC scheme, for the case when a constant speed is assumed for the putative leader. 1st scenario: the putative leader accelerates and then follows a constant speed trajectory (control step: blue = 0.1 s, red = 0.5 s, black = 2.0 s). (For interpretation of the references to colour in this figure legend, the reader is referred to the web version of this article.)

Table 1
The effect of the control step on the cost of the produced trajectory for the case of Fig. 12.

Control step	0.1 s	0.2 s	0.5 s	1.0 s	2.0 s
Cost	17.3	18.7	24.1	38.4	101.4

vehicle (Schmidt and Posch, 2010; Uno et al., 1999; Ntousakis et al., 2014a). Although this control method has the advantage that it does not need a separate controller to react to the putative leader's movement, it can lead to unnecessarily strong accelerations or decelerations. In the following, we use the same leader movement as in Fig. 12 to test the reaction of the ACC merging controller and compare with the optimal control case.

The ACC controller used in this work is the following (Liang and Peng, 1999):

$$a_{des} = K_1(v - v_L) + K_2(x_L - x - v \cdot h_d) \tag{74}$$

where a_{des} is the desired acceleration and v is the speed of the ego vehicle, v_L is the speed of the leader, x is the position of the ego vehicle, x_L is the position of the leader, h_d is the desired time headway and K_1, K_2 are the control gains, with values 1.19 and 1.72, respectively. The desired acceleration is bounded by the maximum acceleration and the maximum deceleration, usually in the range between -4 and 3 m/s^2; moreover, the jerk was also bounded in the range between -3 and 4 m/s^3. The simulation step is equal to 0.01 s, while the control step equals 0.2 s. The produced trajectory using the ACC controller is presented in Fig. 14. It is evident that the merging procedure virtually nullifies the final speed and headway errors, but the produced trajectory features large and abrupt variations in acceleration and jerk, contrary to the smoother ones produced by the proposed methodology. The resulting value of the trajectory cost is 496339.78, which is significantly higher than in the optimal control cases.

5.4. Application to a set of vehicles

In this section, a more general and ordinary application of the proposed methodology is presented; the effectiveness of the proposed methodology is assessed in a scenario where a set of several vehicles exists inside the cooperation area, and all of them follow the proposed methodology. In order to facilitate such a scenario, the following assumptions are adopted:

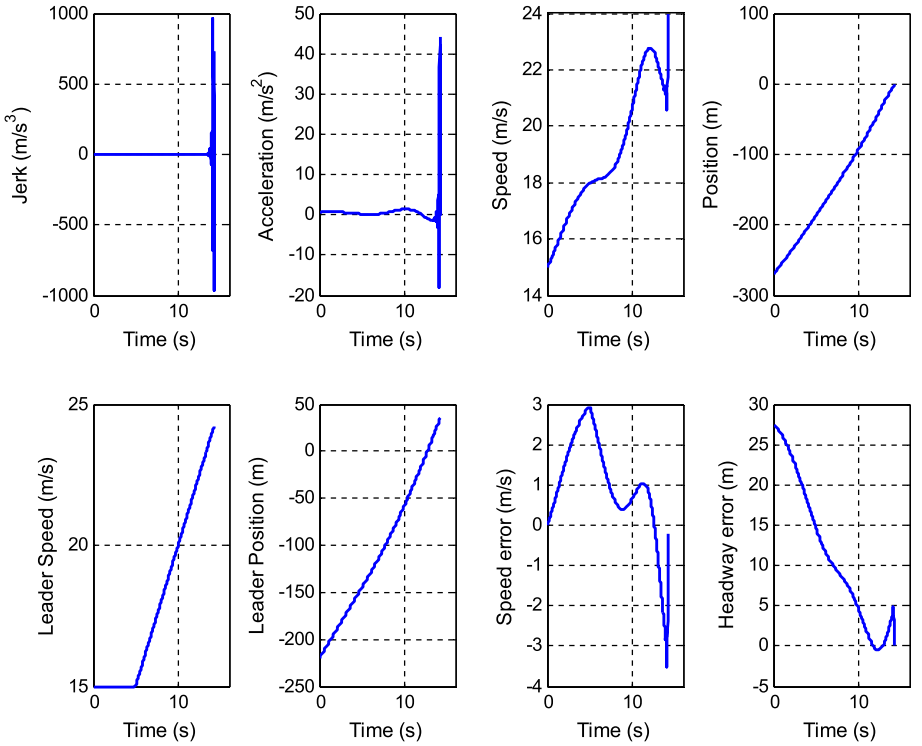

Fig. 13. MPC scheme, for the case when a constant speed is assumed for the putative leader. 2nd scenario: the putative leader accelerates until the merging point (control step: 0.2 s).

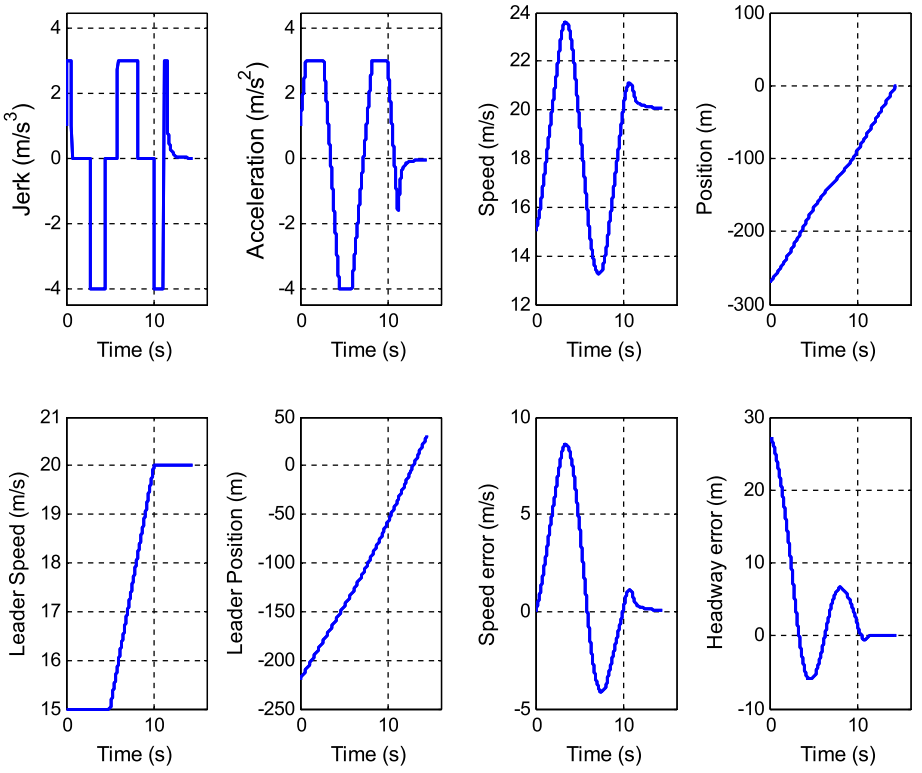

Fig. 14. The produced trajectory using the ACC merging controller.

- An upper control level decides on the merging sequence of the vehicles inside the cooperation area and updates it on a regular basis, in order to deal with disturbances or other unexpected events.
- Each merging vehicle is equipped with a controller that applies the MPC scheme, as described in the previous sections, and computes an optimal trajectory.
- All vehicles are equipped with an ACC controller, which enables the automatic following of their leading vehicles in the same lane (actual leaders). Outside the cooperation area, only the ACC controller is active – for all vehicles.
- The MPC and ACC controllers are simultaneously active, inside the cooperation area, while the command that is actually applied to the vehicle is the most restrictive one. This is necessary in order to guarantee safety.
- No constraints are imposed in this work for the extreme values of jerk, acceleration, and speed (for both controllers - for compatibility reasons).
- The merging control process ends for a vehicle, once it has successfully merged into the mainstream.

Each merging vehicle, in order to be able to apply the proposed methodology, needs two values (at each control step): the expected time of arrival (T) and the expected speed v_e at the merging point, which are provided by its putative leader. Each putative leader continuously transmits the updated information to the corresponding follower vehicle until its merging, for updating the latter's optimal trajectory at every control step.

A flow chart of the MPC methodology for a set of vehicles is presented in Fig. 15.

In the following examples, an application of this methodology to a set of vehicles is presented, to demonstrate: (a) its applicability and practicality, and (b) how the variations in the movement of the putative leader affect the corresponding ego vehicle. Without limiting the generality of the proposed methodology, for simulation purposes we consider a set of 6 vehicles, initially traveling under ACC control, which enter the cooperation area successively (Fig. 16). The merging sequence for this example is pre-defined to be L-A-B-C-D-E (Fig. 16); however, in a real application this MS would be dynamically determined by the upper level controller. We assume that the cooperation area begins 200 m upstream of the merging point. The leading vehicle L is moving with a constant speed.

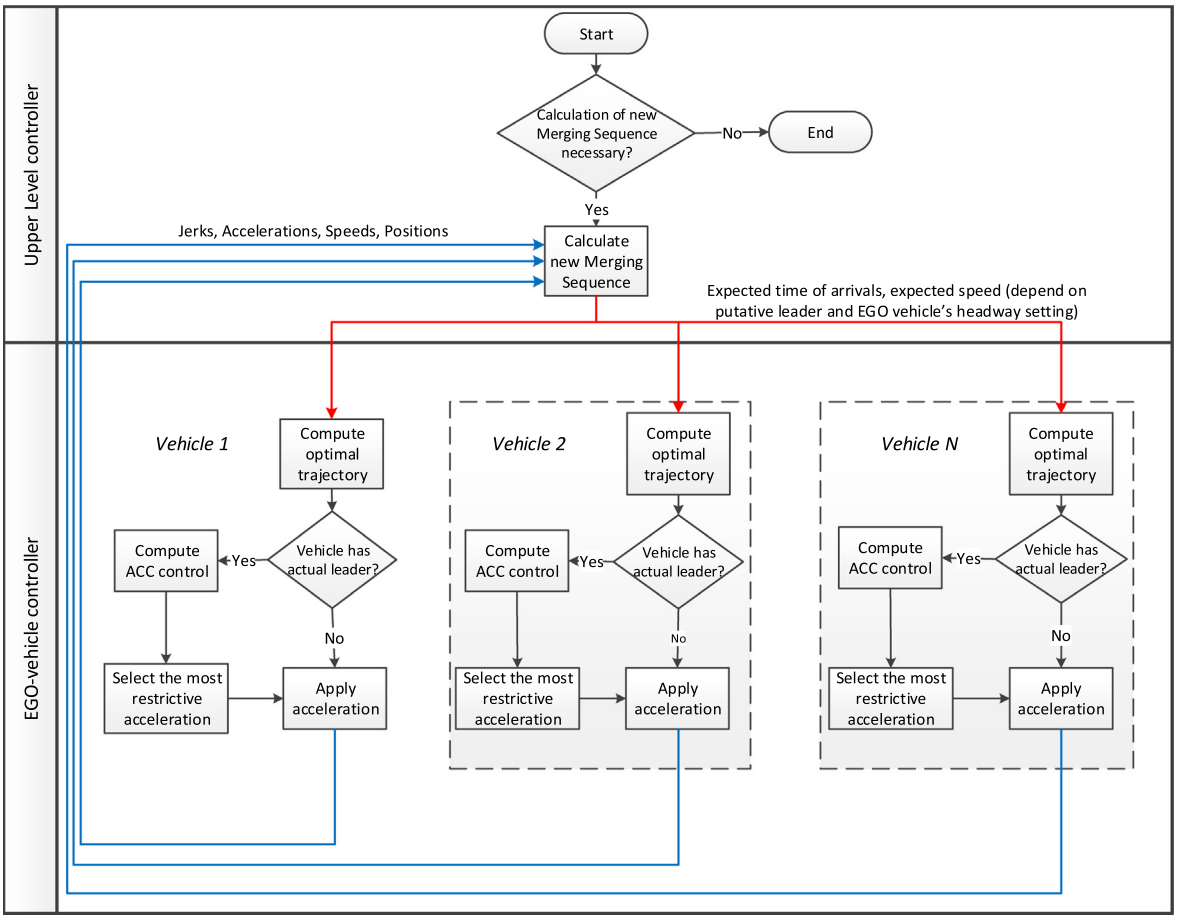

Fig. 15. The flow chart of the MPC methodology applied for a set of vehicles.

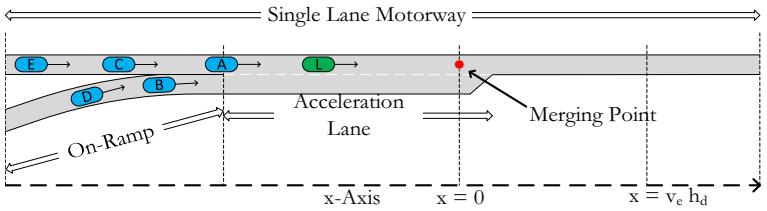

Fig. 16. Representation of the predefined merging sequence for the set of vehicles involved in the automated merging procedure.

Table 2
The initial conditions for the vehicles involved in the test depicted in Fig. 16.

Vehicle ID	L	A	B	C	D	E
Position (m)	−300	−330	−342.5	−360	−368	−390
Speed (m/s)	20	20	17	20	17	20
Acceleration (m/s^2)	0	0	0	0	0	0
Jerk (m/s^3)	0	0	0	0	0	0

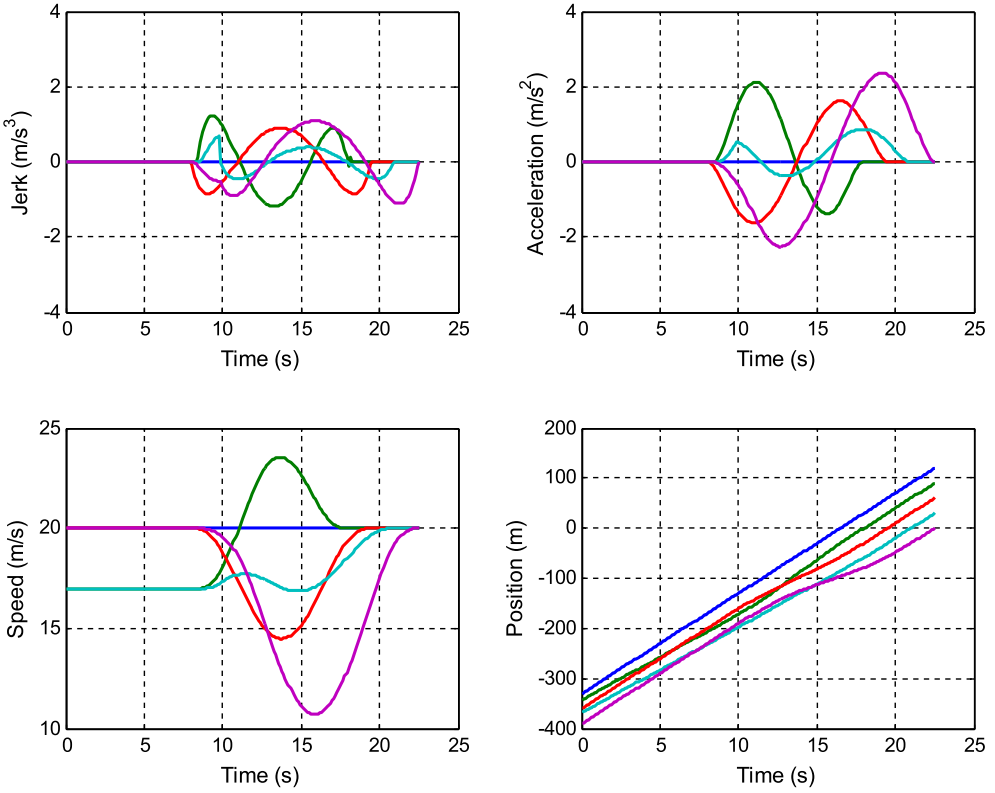

Fig. 17. Application of the MPC scheme to a set of vehicles. 1st scenario: the putative leaders transmit their expected times and speeds at the merging point; vehicles: A: Blue, B: Green, C: Red, D: Light Blue, and E: Purple. (For interpretation of the references to colour in this figure legend, the reader is referred to the web version of this article.)

As previously mentioned, the movement of vehicles is affected by the merging system, only when they are located inside the cooperation area. For this experiment, it is assumed that any vehicle that has no actual and no putative leader travels with acceleration equal to zero. The simulation step was set equal to 0.1 s (same for the ACC controller step), while the control step for the MPC was set to 0.2 s. Table 2 contains the initial conditions for the vehicles involved in the test. The simulation results for the first example are depicted in Fig. 17.

Before commenting on the results of Fig. 17, it should be emphasized that this particular example is a demanding one, since the mainstream vehicles arriving in the cooperation area have already the desired distance with their actual leaders (provided by the active ACC systems). However, in order to allow for the two on-ramp vehicles to merge, the necessary gaps

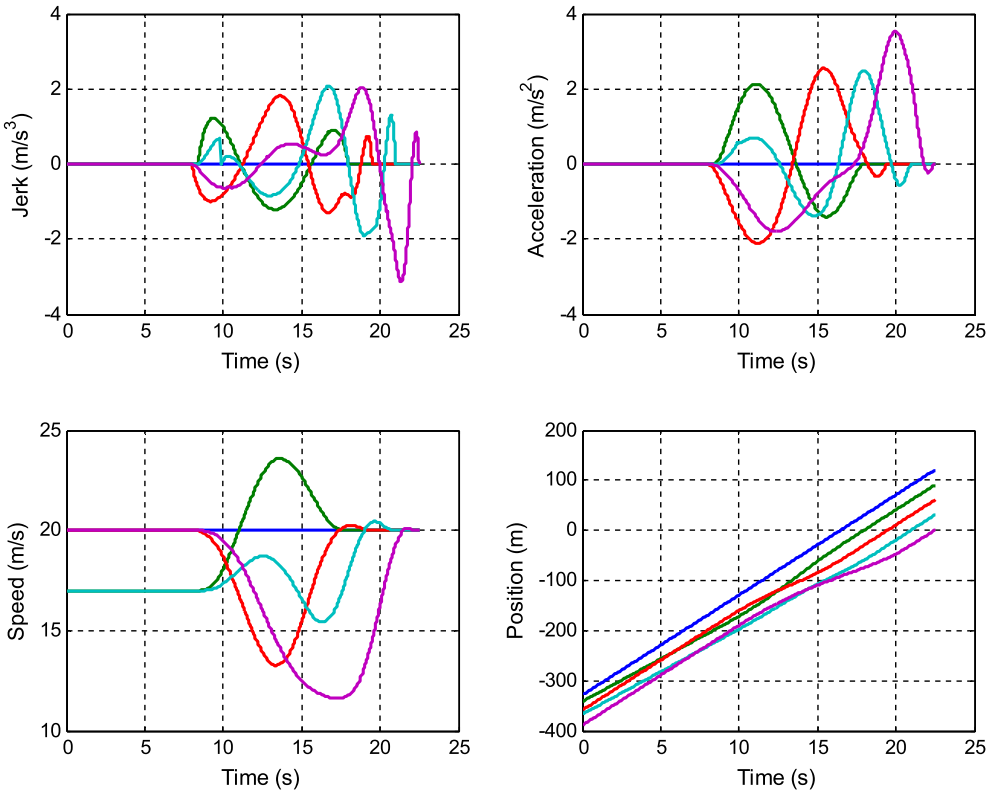

Fig. 18. Application of the MPC scheme to a set of vehicles. 2nd scenario: the putative leaders transmit only their current speeds in each time step; vehicles: A: Blue, B: Green, C: Red, D: Light Blue, and E: Purple. (For interpretation of the references to colour in this figure legend, the reader is referred to the web version of this article.)

should be created; thus, they need to perform a maneuver to first decelerate and, once the gaps are created, accelerate again to reach the speeds of their putative leaders. These maneuvers are automatically (and optimally) created by the proposed optimal control methodology.

In the performed simulation (Fig. 17), the system proves capable to successfully implement the decision of the upper level controller regarding the merging sequence. In other words, the vehicles move on to the downstream section in the prescribed order. Equally importantly, the vehicles merge with the correct speeds and headways. Finally, the average accelerations imposed can be considered acceptable, although in some cases high instantaneous values were unavoidable.

In the second example, the same simulation was performed, considering now that the putative leaders cannot transmit T and v_e but only their current speed and position. The following vehicles predict the values T and v_e, based on the naïve assumption of constant speed for their putative leaders, and continuously re-estimate those values in each time step of the MPC scheme, as described in a previous section. The corresponding simulation results are depicted in Fig. 18.

Similarly to the previous example, the system successfully executes the merging tasks in the correct order. Additionally, the vehicles manage to proceed to the downstream section with the correct speed and headway, although the assumption of constant speed was not close to the real situation. This success is attributed to the use of the MPC controller (in combination with the optimal trajectory specification), which successfully compensates for the resulting errors. However, compared to the previous example, higher values for jerk and acceleration are observed. This is expected, since the actions of the controller are based on an incorrect assumption, and, as the vehicles approach the merging point, less time is available to correct this error. Nevertheless, the application of the proposed methodology for a set of vehicles proved to be applicable and effective, while its extension to any number of interacting vehicles is straightforward.

6. Conclusions

A trajectory planning methodology for the facilitation of an automated merging procedure was proposed, based on an optimal control problem formulation, with analytic solutions. Traffic efficiency is taken into account through the final conditions of the problem, which guarantee that the vehicle will proceed to the downstream section with the correct speed and headway. The cost function to be minimized includes the weighted sum of the squares of the acceleration, jerk and derivative of the jerk. By minimizing this function, passenger comfort and engine effort are directly considered. The resulting analytic optimal solution can be stored in the controller of each vehicle. Only two input values from the vehicle's putative leader are

needed to compute the optimal trajectory, namely the time to the merging point and the final speed at the same position. If an accurate estimation of these input values is not available, the methodology can be applied through a MPC scheme, which can compensate for possible errors. In the case that the putative leader cannot transmit the necessary values to its follower (merging vehicle) in the on-ramp, its current speed and position can be used instead, along with a prediction of its future speed; then, the MPC scheme is used to continuously update the optimal trajectory, based on the updated values provided by the putative leader.

The simulation results proved the applicability and effectiveness of the methodology, and highlighted the importance of having a correct estimation for the input values. The impact of the different weight combinations to the cost function of the optimization problem was also studied, as well as the impact of the control step length for the MPC scheme. In particular, the specification of the cost criterion weights (within a range) might be left to the drivers, according to their possible preferences for more "dynamic" or smoother driving behaviour. The superiority of the proposed methodology with respect to a typical ACC controller was demonstrated; the latter may produce high and abrupt variations of acceleration and jerk, contrary to the much smoother ones produced by the proposed one. It was also shown that the solution of the LQ optimization problem can be given in a feedback form, as a finite horizon linear-quadratic-regulator. This formulation provides certain computational advantages as the required matrices can be computed off-line and stored in the vehicle.

The proposed MPC scheme for a pair of vehicles was finally extended and applied to an arbitrary set of vehicles within the cooperation area, with a prescribed merging sequence. The extended methodology includes the use of an ACC controller for all vehicles, while the MPC is used alongside the ACC inside the cooperation area. Simulation results demonstrate the applicability and effectiveness of the proposed methodology, and its potential for real-world application. Additional tests will be carried out to assess the performance of the proposed methodology in different flow conditions. Moreover, the combination of the proposed methodology with a proper upper-level controller, which facilitates the computation of the merging sequence, is under development.

Acknowledgements

The research leading to these results has received funding from the European Research Council under the European Union's Seventh Framework Programme (FP/2007-2013)/ERC Grant Agreement n. 321132, project TRAMAN21.

Appendix A

A.1. Minimization of acceleration

The analytic expressions for the four constants, defining the analytic solution of the optimal trajectories, are listed below:

$$c_1 = \frac{6}{T^2}(v_e + v_0) + \frac{12x_0}{T^3} \tag{A.1}$$

$$c_2 = -\frac{6x_0}{T^2} - \frac{2v_e + 4v_0}{T} \tag{A.2}$$

$$c_3 = v_0 \tag{A.3}$$

$$c_4 = x_0 \tag{A.4}$$

A.2. Minimization of jerk

The following linear system of equations provides the six constants, defining the analytic solution of the optimal trajectories:

$$x_3(0) = a_0 = -c_4 \tag{A.5}$$

$$x_3(T) = 0 = -\frac{1}{6}c_1T^3 - \frac{1}{2}c_2T^2 - c_3T - c_4 \tag{A.6}$$

$$x_2(0) = v_0 = -c_5 \tag{A.7}$$

$$x_2(T) = v_e = -\frac{1}{24}c_1T^4 - \frac{1}{6}c_2T^3 - \frac{1}{2}c_3T^2 - c_4T - c_5 \tag{A.8}$$

$$x_1(0) = x_0 = -c_6 \tag{A.9}$$

$$x_1(T) = 0 = -\frac{1}{120}c_1T^5 - \frac{1}{24}c_2T^4 - \frac{1}{6}c_3T^3 - \frac{1}{2}c_4T^2 - c_5T - c_6 \tag{A.10}$$

A.3. Minimization of jerk's derivative

The following linear system of equations provides the eight constants, defining the analytic solution of the optimal trajectories:

$$x_4(0) = j_0 = c_5 \tag{A.11}$$

$$x_4(T) = 0 = \frac{c_1T^4}{24} + \frac{c_2T^3}{6} + \frac{c_3T^2}{2} + c_4T + c_5 \tag{A.12}$$

$$x_3(0) = a_0 = c_6 \tag{A.13}$$

$$x_3(T) = 0 = \frac{c_1T^5}{120} + \frac{c_2T^4}{24} + \frac{c_3T^3}{6} + \frac{c_4T^2}{2} + c_5T + c_6 \tag{A.14}$$

$$x_2(0) = v_0 = c_7 \tag{A.15}$$

$$x_2(T) = v_e = \frac{c_1T^6}{720} + \frac{c_2T^5}{120} + \frac{c_3T^4}{24} + \frac{c_4T^3}{6} + \frac{c_5T^2}{2} + c_6T + c_7 \tag{A.16}$$

$$x_1(0) = x_0 = c_8 \tag{A.17}$$

$$x_1(T) = 0 = \frac{c_1T^7}{5040} + \frac{c_2T^6}{720} + \frac{c_3T^5}{120} + \frac{c_4T^4}{24} + \frac{c_5T^3}{6} + \frac{c_6T^2}{2} + c_7T + c_8 \tag{A.18}$$

A.4. Minimization of the combined cost function

The following linear system of equations provides the eight constants, defining the analytic solution of the optimal trajectories for this case:

$$x_4(0) = j_0 = \frac{c_1}{w_1} + c_5 \cdot A_1^3 - c_6 \cdot A_1^3 + c_7 \cdot A_2^3 - c_8 \cdot A_2^3 \tag{A.19}$$

$$x_4(T) = 0 = \frac{c_1}{w_1} + c_5 \cdot A_1^3 \cdot e^{A_1*T} - c_6 \cdot A_1^3 \cdot e^{-A_1*T} + c_7 \cdot A_2^3 \cdot e^{A_2*T} - c_8 \cdot A_2^3 \cdot e^{-A_2*T} \tag{A.20}$$

$$x_3(0) = a_0 = \frac{c_2}{w_1} + c_5 \cdot A_1^2 + c_6 \cdot A_1^2 + c_7 \cdot A_2^2 + c_8 \cdot A_2^2 \tag{A.21}$$

$$x_3(T) = 0 = \frac{c_2}{w_1} + \frac{c_1}{w_1}T + c_5 \cdot A_1^2 \cdot e^{A_1*T} + c_6 \cdot A_1^2 \cdot e^{-A_1*T} + c_7 \cdot A_2^2 \cdot e^{A_2*T} + c_8 \cdot A_2^2 \cdot e^{-A_2*T} \tag{A.22}$$

$$x_2(0) = v_0 = \frac{c_3}{w_1} + \frac{c_1w_2}{w_1^2} + c_5 \cdot A_1 - c_6 \cdot A_1 + c_7 \cdot A_2 - c_8 \cdot A_2 \tag{A.23}$$

$$x_2(T) = v_e = \frac{c_3}{w_1} + \frac{c_2}{w_1}T + \frac{c_1w_2}{w_1^2} + \frac{c_1}{2w_1}T^2 + c_5 \cdot A_1 \cdot e^{A_1*T} - c_6 \cdot A_1 \cdot e^{-A_1*T} + c_7 \cdot A_2 \cdot e^{A_2*T} - c_8 \cdot A_2 \cdot e^{-A_2*T} \tag{A.24}$$

$$x_1(0) = x_0 = \frac{w_2c_2}{w_1^2} + \frac{c_4}{w_1} + c_5 + c_6 + c_7 + c_8 \tag{A.25}$$

$$x_1(T) = 0 = \frac{w_2c_1}{w_1^2}T + \frac{w_2c_2}{w_1^2} + \frac{c_1}{6w_1}T^3 + \frac{c_2}{2w_1}T^2 + \frac{c_3}{w_1}T + \frac{c_4}{w_1} + c_5 \cdot e^{A_1*T} + c_6 \cdot e^{-A_1*T} + c_7 \cdot e^{A_2*T} + c_8 \cdot e^{-A_2*T} \tag{A.26}$$

where

$$A_1 = \sqrt{\frac{w_2 - \sqrt{w_2^2 - 4w_1}}{2}} \tag{A.27}$$

$$A_2 = \sqrt{\frac{w_2 + \sqrt{w_2^2 - 4w_1}}{2}} \tag{A.28}$$

References

Athans, M., 1969. A unified approach to the vehicle-merging problem. Transp. Res. 3 (1), 123–133.

Cao, W., Muka, M., Kawabe, T., Nishira, H., Fujiki, N., 2014. Merging trajectory generation for vehicle on a motorway using receding horizon control framework consideration of its applications. In: Proceedings of the 2014 IEEE conference on control applications, pp. 2127–2134. http://dx.doi.org/10.1109/CCA.2014.6981617.

Davis, L.C., 2006. Effect of cooperative merging on the synchronous flow phase of traffic. Physica A 361 (2), 606–618. http://dx.doi.org/10.1016/j.physa.2005.06.046.

Davis, L.C., 2007. Effect of adaptive cruise control systems on mixed traffic flow near an on-ramp. Physica A 379 (1), 274–290. http://dx.doi.org/10.1016/j.physa.2006.12.017.

Elbanhawi, M., Simic, M., Jazar, R., 2015. In the passenger seat: investigating ride comfort measures in autonomous car. IEEE Intell. Transp. Syst. Mag. 7 (3), 4–17. http://dx.doi.org/10.1109/MITS.2015.2405571.

Kachroo, P., Li, Z., 1997. Vehicle merging control design for an automated highway system. In: Proceedings of the IEEE Conference on Intelligent Transportation Systems, pp. 224–229, doi:10.1109/ITSC.1997.660479.

Kesting, A., Treiber, M., Schönhof, M., Helbing, D., 2008. Adaptive cruise control design for active congestion avoidance. Transp. Res. Part C 16 (6), 668–683. http://dx.doi.org/10.1016/j.trc.2007.12.004.

Li, L., Wang, F.-Y., Zhang, Y., 2007. Cooperative driving at lane closures. In: Proceedings of the 2007 IEEE Intelligent Vehicles Symposium, Istanbul, Turkey, pp. 1156–1161. http://dx.doi.org/10.1109/IVS.2007.4290274.

Liang, C.-Y., Peng, H., 1999. Optimal adaptive cruise control with guaranteed string stability. Veh. Syst. Dynam.: Int. J. Veh. Mech. Mob. 32 (4–5), 313–330. http://dx.doi.org/10.1076/vesd.32.4.313.2083.

Lu, X.Y., Tan, H.S., Shladover, S.E., Hedrick, K.J., 2004. Automated vehicle merging maneuver implementation for AHS. Veh. Syst. Dynam.: Int. J. Veh. Mech. Mob. 41 (2), 85–107. http://dx.doi.org/10.1076/vesd.41.2.85.26497.

Marczak, F., Daamen, W., Buisson, C., 2013. Merging behaviour: empirical comparison between two sites and new theory development. Transp. Res. Part C 36, 530–546. http://dx.doi.org/10.1016/j.trc.2013.07.007.

Marinaki, M., Papageorgiou, M., 2005. Optimal Real-Time Control of Sewer Networks. Springer-Verlag, London. http://dx.doi.org/10.1007/b138719.

Mattingley, J., Wang, Y., Boyd, S., 2011. Recending horizon control. Automatic generation of high-speed solvers. IEEE Control Syst. Magaz. 31 (3), 52–65. http://dx.doi.org/10.1109/MCS.2011.940571.

Milanés, V., Godoy, J., Villagrá, J., Pérez, J., 2011. Automated on-ramp merging system for congested traffic situations. IEEE Trans. Intell. Transp. Syst. 12 (2), 500–508. http://dx.doi.org/10.1109/TITS.2010.2096812.

Ntousakis, I.A., Porfyri, K., Nikolos, I.K., Papageorgiou, M., 2014a. Assessing the impact of a cooperative merging system on highway traffic using a microscopic flow simulator. In: Proceedings of the ASME 2014 International Mechanical Engineering Conference & Exposition, IMECE2014, Montreal, Quebec, Canada, vol. 12: Transportation Systems, Paper No. IMECE2014-39850. doi:http://dx.doi.org/10.1115/IMECE2014-39850.

Ntousakis, I.A., Nikolos, I.K., Papageorgiou, M., 2014b. On microscopic modelling of Adaptive Cruise Control systems. In: 4th International Symposium of Transport Simulation, ISTS 2014, Corsica, France, doi:http://dx.doi.org/10.1016/j.trpro.2015.03.010 (Published in Transp. Res. Proc. 6, 111–127).

Papageorgiou, M., Leibold, M., Buss, M., 2012. Optimierung - Statische, Dynamische, Stochastische Verfahren Für Die Anwendung (Optimisation – Applied Static, Dynamic, Stochastic Methods), third ed. (revised and updated). Springer, Berlin.

Park, H., Bhamidipati, C.S., Smith, B.L., 2011. Development and evaluation of enhanced IntelliDrive-Enabled lane changing advisory algorithm to address freeway merge conflict. Transp. Res. Record: J. Transp. Res. Board 2243, 146–157. http://dx.doi.org/10.3141/2243-17.

Posch, B., Schmidt, G., 1983. A comprehensive control concept for merging of automated vehicles under a broad class of traffic conditions. In: Klamt, D., Lauber, R. (Eds.), Control in Transportation Systems, Proceedings of the 4th IFAC/IFIP/IFORS Conference, Baden-Baden, Germany, pp. 187–194.

Pueboobpaphan, R., Liu, F., van Arem, B., 2010. The impacts of a communication based merging assistant on traffic flows of manual and equipped vehicles at an on-ramp using traffic flow simulation. In: Proceedings of the 13th International IEEE Conference on Intelligent Transportation Systems, Madeira Island, Portugal, pp. 1468–1473. http://dx.doi.org/10.1109/ITSC.2010.5625245.

Ran, B., Leight, S., Chang, B., 1999. A microscopic simulation model for merging control on a dedicated-lane automated highway system. Transp. Res. Part C 7 (6), 369–388. http://dx.doi.org/10.1016/S0968-090X(99)00028-5.

Raravi, G., Shingde, V., Ramamritham, K., Bharadia, J., 2007. Merge algorithms for intelligent vehicles. In: Sampath, P., Ramesh, S. (Eds.), Next Generation Design and Verification Methodologies for Distributed Embedded Control Systems. Springer, pp. 51–65.

Rathgerber, C., Winkler, F., Kang, X., Müller, S., 2015. Optimal trajectories for highly automated driving. Int. J. Mech., Indust., Mechat. Manuf. Eng. 9 (6), 946–952.

Rios-Torres, J., Malikopoulos, A.A., Pisu, P., 2015. Online optimal control of connected vehicles for efficient traffic flow at merging roads. In: Proceedings of the 2015 IEEE 18th International Conference on Intelligent Transportation Systems, Las Palmas, Gran Canaria, Spain, pp. 2432–2437. http://dx.doi.org/10.1109/ITSC.2015.392.

Roncoli, C., Papageorgiou, M., Papamichail, I., 2015a. Traffic flow optimisation in presence of vehicle automation and communication systems – Part II: optimal control for multi-lane motorways. Transp. Res. Part C 57, 260–275. http://dx.doi.org/10.1016/j.trc.2015.05.011.

Roncoli, C., Papamichail, I., Papageorgiou, M., 2015. Model predictive control for motorway traffic with mixed manual and VACS-equipped vehicles. In: 18th EURO Working Group on Transportation Meeting (EWGT 2015), 14–16 July 2015, Delft, The Netherlands, doi:http://dx.doi.org/10.1016/j.trpro.2015.09.095 (Published in Transp. Res. Proc. 10, 452–461).

Scarinci, R., Heydecker, B., 2014. Control concepts for facilitating motorway on-ramp merging using intelligent vehicles. Transp. Rev.: A Transnat. Transdisc. J. 34 (6), 775–797. http://dx.doi.org/10.1080/01441647.2014.983210.

Schmidt, G., Posch, B., 2010. Automatische Zusammmenführung zweier Fahrzeugströme – eine Rückblende. Automatisierungstechnik 58 (6), 317–321. http://dx.doi.org/10.1524/auto.2010.0842.

Sun, J., Ouyang, J., Yang, J., 2014. Modeling and analysis of merging behavior at expressway on-ramp bottlenecks. Transp. Res. Rec.: J. Transp. Res. Board 2421, 74–81. http://dx.doi.org/10.3141/2421-09.

Tideman, M., van der Voort, M.C., van Arem, B., Tillema, F., 2007. A review of lateral driver support systems. In: Proceedings of the 2007 IEEE Intelligent Transportation Systems Conference, Seatle, WA, USA, pp. 992–999. http://dx.doi.org/10.1109/ITSC.2007.4357753.

Uno, A., Sakaguchi, T., Tsugawa, S., 1999. A merging control algorithm based on inter-vehicle communication. In: Proceedings of the IEEE/IEEJ/JSAI International Conference on Intelligent Transportation Systems, pp. 783–787. doi:http://dx.doi.org/10.1109/ITSC.1999.821160.